AD-A120 551 VPE GROWTH OF INP FOR ELECTRONIC DEVICES(U) WASHINGTON 1/2
UNIV ST LOUIS MO DEPT OF ELECTRICAL ENGINEERING
J M BORNHOLDT ET AL. MAY 82 82-2-ONR N00014-79-C-0840
UNCLASSIFIED F/G 9/5 NL

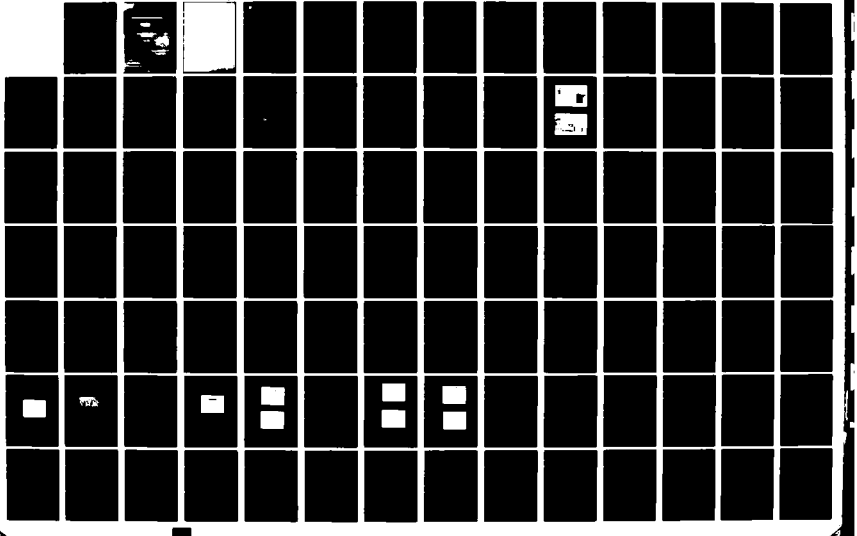

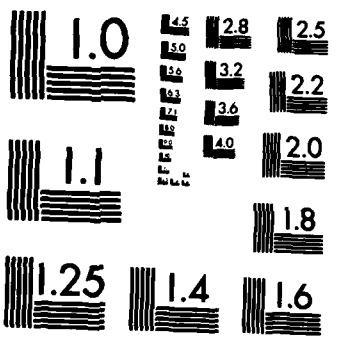

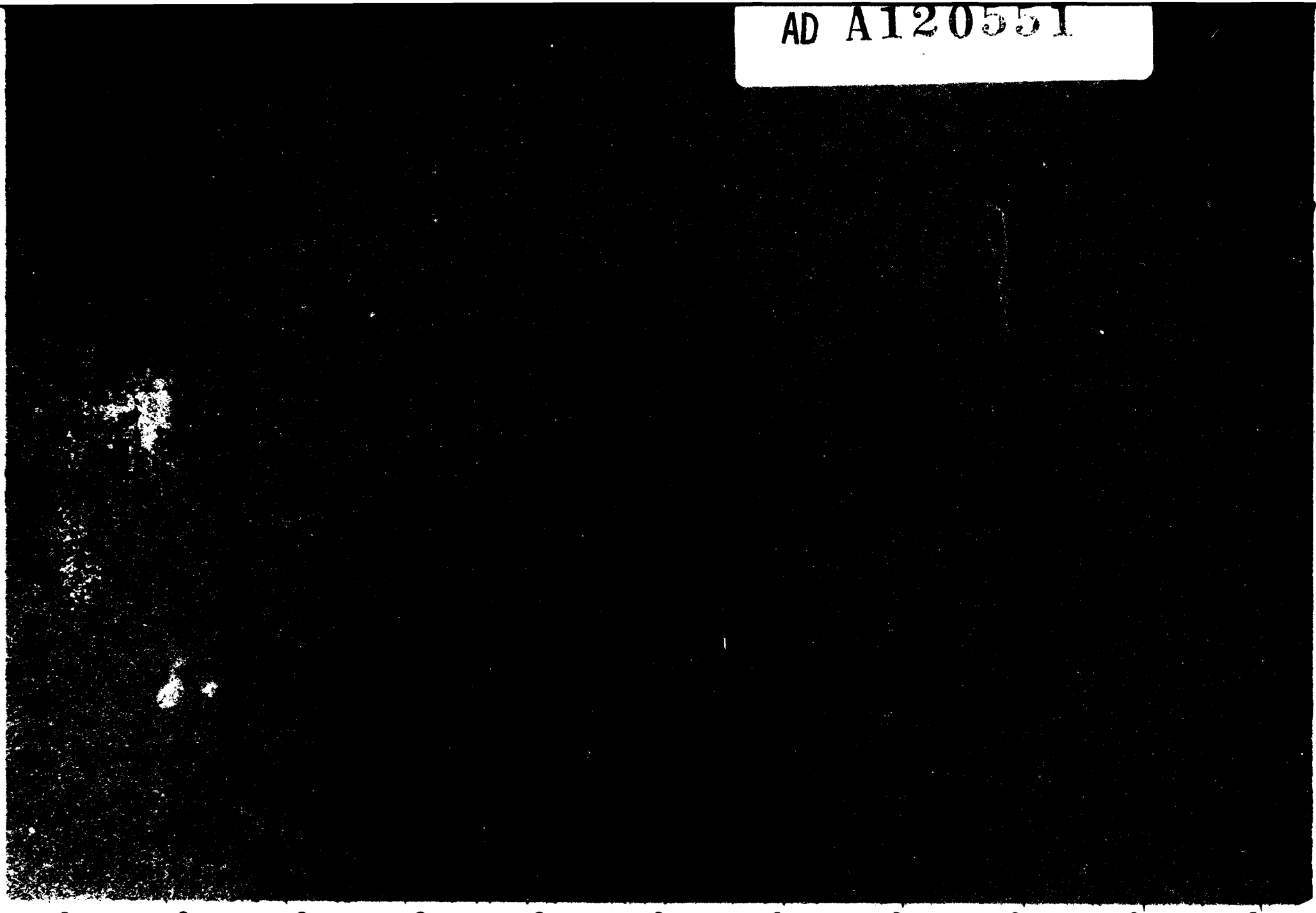

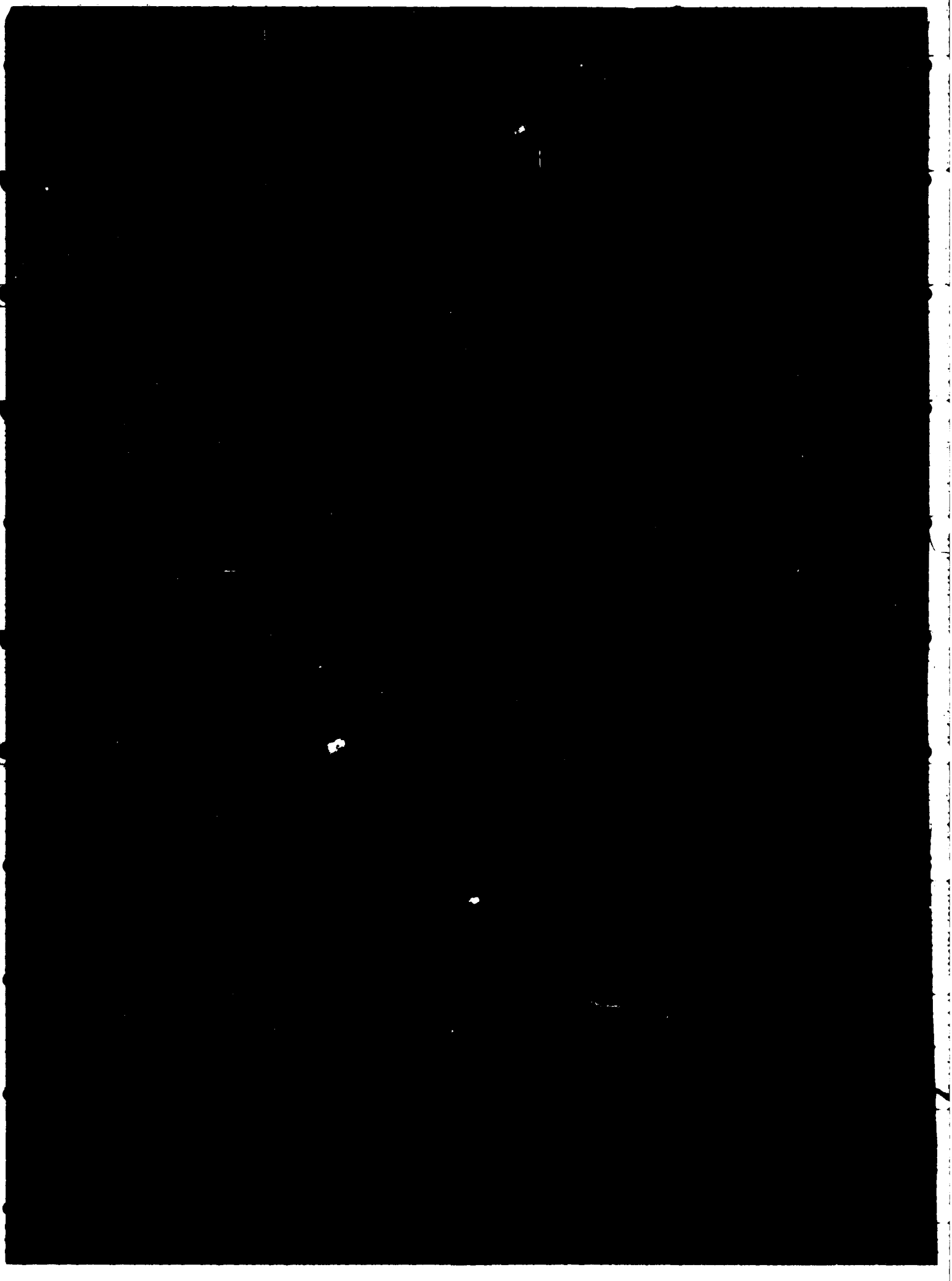

WASHINGTON UNIVERSITY IN ST. LOUIS

VPE Growth of InP For Electronic Devices

J.M. BORNHOLDT
R.E. GOLDWASSER
F.J. ROSENBAUM

Department of Electrical Engineering
Washington University
St. Louis, Mo. 63130

May 1982

Technical Report ONR-82-2

Office of Naval Research
Arlington, VA. 22217

Contract: N00014-79-C-840
Contract Authority: NR SR0-004

TABLE OF CONTENTS

TABLE OF CONTENTS
(continued)

TABLE OF CONTENTS
(continued)

LIST OF TABLES

LIST OF FIGURES

LIST OF FIGURES
(continued)

VPE GROWTH OF InP FOR ELECTRONIC DEVICES

1. INTRODUCTION

Indium Phosphide is a semiconductor compound with attractive possibilities for millimeter wave applications. The peak to valley ratio, peak electron velocity, and thermal conductivity of the material are all higher than those of GaAs [1].* Theoretically, it should be possible to fabricate superior devices at higher frequencies with InP [2,3,4]. Consequently there is great interest in producing device grade InP in order to study its properties in known devices and to fabricate new devices with it [1-7].

1.1 HISTORICAL PERSPECTIVE

Although technology for the growth and fabrication of InP is not as advanced as for GaAs, major strides have been made in the last decade. Among others, R. C. Clarke [4,5,8] has performed extensive work on the PCL_3-In-H_2 process, commonly used for the vapor phase epitaxial (VPE) growth of InP [1,8]. In this process a controlled concentration of phosphorous trichloride (PCl_3) vapor in hydrogen is passed over indium at temperatures between 700°C and 750°C. The products, indium monochloride and phosphorous vapor, pass over polished seed wafers at 650°C where epitaxy of InP occurs [4]. The growth rate and impurity concentration of the material depend upon the purity of

* The numbers in parentheses in the text indicate references in the Bibliography.

the raw materials and the growth conditions employed. These growth conditions can be controlled to produce thin layers of semiconductor suitable for electronic devices. In addition, the epitaxial material may be intentionally doped to provide a desired profile of electron concentration versus depth in the crystal.

Clarke [4] has found that three interrelated factors influence the growth rate and impurity incorporation rate during epitaxial deposition: (1) The temperature gradient across the source, (2) the PCl_3 mole fraction and (3) the indium to phosphorous ratio over the seed. He has obtained epitaxial InP with residual doping levels below 1×10^{-13} cm^{-3} and has also produced narrow highly doped layers less than 300°A thick using advanced doping techniques [9].

Others have also successfully grown InP and fabricated devices as well. In 1979 Moutow, Chevrier, Huber, and Montel experimented with various growth parameters and fabricated millimeter wave oscillators which generated 60-80 mW at 60 Ghz with a 2-3% efficiency [6]. Morkoc, Andrews, Hyder, and Bandy [7] reported fabrication of InP Schottky barrier field-effect transistors (MESFETS) with gate dimensions of $1.2 \times 200\mu m$ and $7\mu m$. Their VPE material had residual background concentration less than 10^{14} cm^{-3}, and n-type material doped to 10^{15} cm^{-3} showed a 77°K mobility of greater than 40,000 cm^2/Vs. The devices had a maximum power gain cutoff frequency of 30 Ghz compared with 21 Ghz for similar GaAs devices. A maximum available gain of 15dB and minimum noise figure of 3dB (with associated gain of about 8dB) at 6.6 Ghz were measured. Chevier, Armand, Huber, and Link [2] also fabricated MESFETS, reporting "encouraging" static characteristics (I_{DD} = 24mA, g_m = 19 mS

for a gate of 2 μm by 200 μm). They noted that "although the InP technologies are not as advanced as GaAs, experimental data already show that the cut-off frequency is higher in InP than in GaAs" [2].

As the technologies for InP growth and device fabrication improve so will the performance of associated devices. In fact, as Morkoc observed in 1979, "with the advancements in InP epitaxy, particularly in VPE and also in transferred-electron device technology, which requires n^+ substrates, the millimeter wave application is now dominated by InP" [7]. The material holds great promise.

The technology for InP is far from mature, however. The interdependences of all growth parameters have not been entirely sorted out even though many general trends have been observed. Since the kinetics are different for each individual reactor, direct comparison of results in the literature is not always simple. Results from one worker may not apply to others because of changes in reactor design or growth conditions.

Device fabrication problems also exist, especially with forming adequate Schottky diodes. The barrier height of an InP/metal contact is often very low (.2 or .3eV) and displays little dependence on the work function of the metal employed [9-16]. By 1977 several workers [9-16] had achieved improvements in these contacts by use of a thin interfacial oxide layer between the metal and semiconductor. Since then several techniques for creating a controlled interfacial layer have been reported including etching [10,14] and sintering [13]. Metal rectifying junctions with effective barrier heights around .53eV or greater are possible today [9] as is control of the barrier height

via changes in the oxide layer thickness [12,15]. Clearly, this contact technology is improving.

Since InP technology for growth and device fabrication is rapidly growing, any empirical results concerning either growth or fabrication of InP devices helps further the technology by serving as useful bases for future workers. Along with techniques for epitaxial growth and device fabrication, data is also needed on physical characteristics of the material. One important property of the material is the relationship between the electron velocity and the electric field, which is essential for accurate device modeling. A system for measuring the electron velocity versus the electric field was constructed at Washington University in 1980 [17]. It has already been used to measure the transport properties of GaAs [18] and will be used to measure those of InP. Therefore, a specific need exists to fabricate a special InP device which can be used in this system to measure its transport properties. Our present growth effort is aimed at providing such a sample.

1.2 SCOPE OF WORK

The purpose of this study is to investigate the problems associated with growing and evaluating device grade InP by constructing a complex vapor phase epitaxial InP growth system, growing controlled layers of InP on n+ substrates, and evaluating the results. The ultimate objectives of the program are fabrication of a special Schottky diode to be used in a system that measures the transport properties of different semiconductors [17] and production of epitaxial InP for use in other devices.

The first phase of the project (Chapter 2) involved the design and construction of a vapor phase epitaxial growth system. The system uses the well known PCl_3-In-H_2 process first used by Clarke [8] and further refined by others. This process is known to reliably produce pure crystals and device grade material [4]. Our particular system employs double dilution doping with H_2S to achieve accurately controlled low doping concentrations and a rolling furnace to achieve rapid warm up and cool down periods during growth. Attempts have been made to make the complex flow system simple to use and easy to maintain, so that it can be used by several people over a long period of time. Efforts were directed towards reduction of impurities in the system and to control of the physical growth processes which cause variations in electrical properties.

The next phase of the study (Chapter 3) was use of the system to grow epitaxial layers of InP on n+ substrates that could be used in devices. The particular responses of the system to various parameters such as source and seed temperatures, PCl_3 mole fraction, and flow rate were investigated. The physical and electrical properties of the grown layers were evaluated. The physical evaluations were found to be straight-forward but attempts to evaluate the electrical properties by C-V analysis revealed problems with fabricating Schottky-barriers on InP.

The problem of poor Schottky diodes presented immediate difficulties in measuring the electrical properties of the layer by C-V techniques. Schottky barriers are also essential for use in many devices, including the one intended for use in the transport measurements.

Therefore it was essential to investigate this problem and find an acceptable solution. Research revealed that use of metal-insulator-semiconductor (MIS) contacts provide an answer. Insertion of a thin layer of oxide between the metal and semiconductor results in a contact that behaves like a simple Schottky barrier with a barrier height up to 0.5eV. Use of different metals and the effect of heat treatment on the effective barrier height of MIS Schottky diodes were also investigated.

In general, many of the common problems of growing a III-V semiconductor have been encountered along with particular problems associated with InP. Solutions have been found to most of these problems. The results contained in this study can be used to refine the reactor to produce purer, more controlled layers of indium phosphide and to assist in fabricating a sample for the v(E) measurements.

2. REACTOR DESIGN AND CONSTRUCTION

Two important factors in the design and construction of a VPE InP reactor system are accurate control of growth parameters and reduction of residual impurities. Such a system must regulate and combine the flow of various gases and maintain a precise temperature profile across the reactor tube prior to and during each growth run. It should be free of residual impurities and gas leaks in order to obtain high purity material but offer the capability for controlled doping of the epitaxial material for device applications.

A reactor system has been implemented which controls the significant growth parameters. Gas flows are regulated by electronic mass flow controllers and rotometers. A rolling furnace serves to maintain a known temperature profile across the reactor tube. A wide range of doping levels can be achieved by use of a double dilution dopant system. In addition, care has been taken in design and construction to minimize residual impurities and the possibility of gas leakage. The reactor discussed in this chapter has been used to grow high purity epitaxial InP as discussed in later chapters.

2.1 REACTOR DESIGN

The major features of the reactor are a double dilution dopant system and a rolling furnace. The double dilution insures accurate control even at very doping low levels. The rolling furnace allows rapid heating and cooling of the reactor to avoid etching problems associated with long heat up or cooling times. A schematic of the reactor is shown in Figure 1.

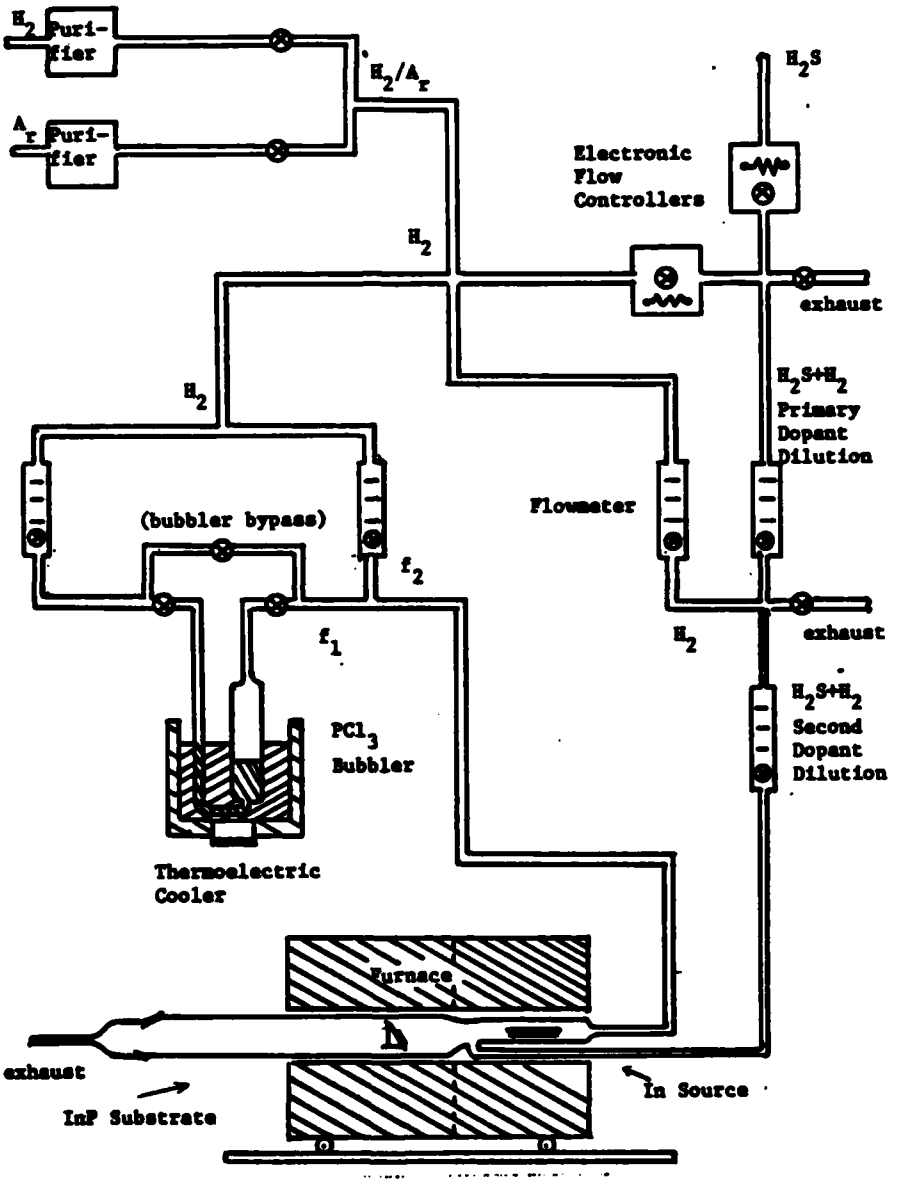

Figure 1. Schematic of the $PCl_3/In/H_2$ V.P.E. System

2.1.1 H_2/Ar Flows

Hydrogen is used as the carrier gas for the InP reactions during melt saturation and growth runs. However, when the tube is opened for maintenance the H_2 flow must be replaced by Ar. This precaution is necessary because white or yellow phosphorus produced during the reaction will spontaneously ignite in the presence of oxygen. The flame from this reaction will ignite the hydrogen and damage the reactor. The introduction of an inert carrier gas such as argon will prevent potential explosions. To insure that only hydrogen flows during growth runs and only argon flows during reactor maintenance loading, a pair of air controlled bellows valves, one "normally open" and the other "normally closed", are controlled by a single N_2 valve which is switched for either "hydrogen" or "argon". This setup insures that only one or the other is on at any given time. The H_2 line is diverted into either the dopant dilution system or the PCl_3 bubbler.

2.1.2 Control of Mole Fraction

The mole fraction of PCl_3 in the H_2 flow is controlled by the temperature of the liquid PCl_3 and by a dilution after the bubbler. The temperature of the PCl_3 is maintained by a thermoelectric cooler. Here Peltier cells act as heat pumps which take heat directly out of the PCl_3 bath into a water cooled heat sink. An Omega RTD digital temperature controller cycles the thermoelectric cells to maintain a constant temperature in the bath. The water in the bath is stirred to minimize thermal gradients. The bath temperature is set to 14.6°C with a deviation less than $\pm$ .05°C.

At 14.6°C PCl_3 has a high vapor pressure that gives a high mole fraction of PCl_3 in the H_2 stream if not dilution is included. Therefore pure H_2 is introduced after the bubbler to further decrease the mole fraction. A wide range of possible PCl_3 mole fractions are possible with this arrangement. This H_2/PCl_3 mixture is introduced into the tube upstream from the source.

The bubbler is switched on and off by a set of air controlled bellows valves similar to the ones used for the H_2/Ar selector. A single N_2 valve indirectly opens or closes the lines to the bubbler while closing or opening the bypass simultaneously. This minimizes the mechanical stress on the bubbler glass-to-metal seals and insures the either-or relationship of bubbler to bypass.

2.1.3 Dopant Dilution System

The dopant, H_2S, is introduced into the system and immediately mixed with pure H_2 to a desired dilution. Both the primary H_2S and H_2 flows are controlled by electronic flow controllers. Part of this mixture is vented into the exhaust line so that the total flow can be easily regulated. The first mixture is again diluted with pure H_2. This final dilution is sent into the reaction tube downstream from the source but upstream from the seed. Rotometers are used to control the flows for the second dilution. Low dilutions can be controlled quite accurately by this method. Refer to Appendix 8.2 for more details.

2.1.4 Furnace

The furnace has two temperature zones which can be separately controlled. One zone sets the source temperature, the other the seed

temperature. The furnace is mounted on a roller track so that it can be easily rolled over a portion of the quartz furnace tube.

A portable exhaust hood is positioned over the end of the furnace tube that is opened for maintenance. This serves as a vent for any gasses that are flushed from the tube during maintenance and ensures a net outward flow of argon from the tube to reduce the possibility of contamination from back flow of atmospheric gas into the tube.

2.2 REACTOR CONSTRUCTION

The reactor was constructed to optimize cleanliness and tightness against leaks so as to minimize residual impurities. After initial construction the system was dismantled, the quartz and pyrex parts cleaned thoroughly in aqua regia and rinsed in deionized water, the stainless steel and aluminum tubes cleaned with trichloroethylene, acetone, and isopropyl and dried in a nitrogen flow. All Swagelock connectors, valves, flow controllers, and rotometers were disassembled, cleaned with acetone and isopropyl, and dried with nitrogen. This procedure removes most surface impurities introduced in glassblowing or manufacturing.

The system was then checked for leaks. Two methods were used. The first was to pass gas through the system and detect leaks using "Snoop". To detect smaller leaks the system was pumped down to vacuum levels and a helium detector employed. The complexity of the system results in a large number of joints which increases the possibility of a leak; therefore it is important that the system is totally leak tested in the construction stage to avoid later complications.

All the gas lines except the dopant system lines are stainless steel. The lines in the dopant system are aluminum because of the corrosive effect hydrogen sulfide has on stainless steel. The reactor tube, seed holder, and melt boat are made of fused quartz. The PCl_3 bubbler is pyrex.

A control panel and power supply for the electronic mass flow controllers were constructed. A $\pm$ 15 volt power supply is used to power the controllers and to create a 0. to 5. volt control voltage that sets the amount of mass flow through the controller. Digital meters are calibrated to read and display an output voltage from the controller corresponding to the actual flow.

Because the vapor pressure of PCl_3 is highly dependent on temperature a special thermoelectric cooler was constructed to maintain a constant and known temperature. This cooler is quite simple, considerably cheaper than a water circulator, and maintains the temperature of the bath very well. Refer to Appendix 8.4.1 for a schematic.

2.3 COMPLETE LAYOUT

The complete system is laid out in a manner which minimizes the amount of space occupied but maximizes user efficiency. The flow controls and monitors are mounted on a vertical control panel as shown in Figure 2. They are all labeled to insure easy use and provide standard notation for documentation.

The mass flow controllers, bellow valves, and rotometers, which are bolted to the back of the control panel and connected by the aluminum and stainless steel tubing, are laid out in a manner which minimizes the number of connections required and so the possibility of

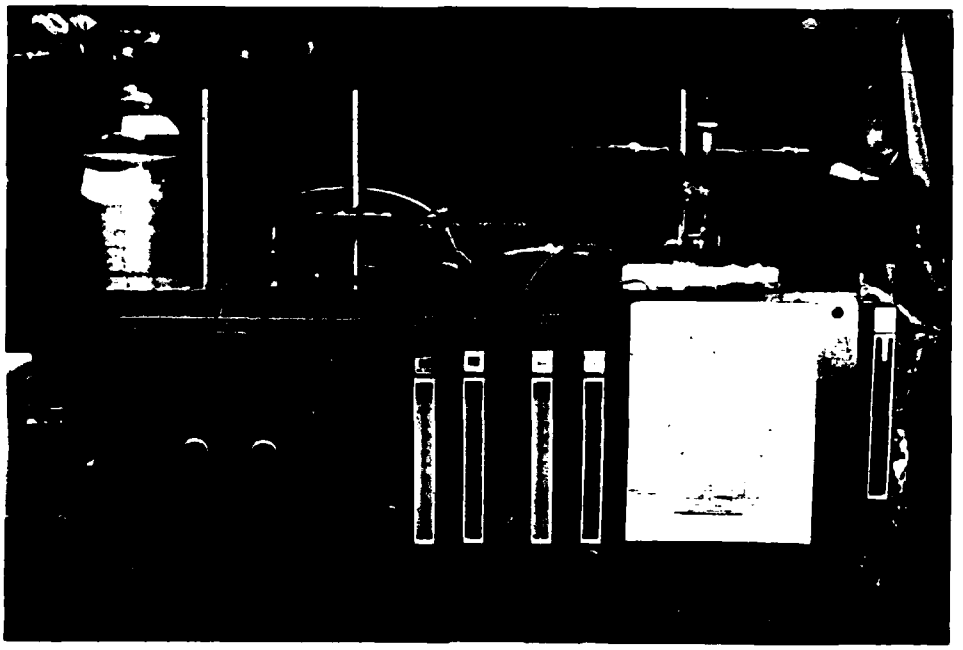

Figure 2. Main control panel

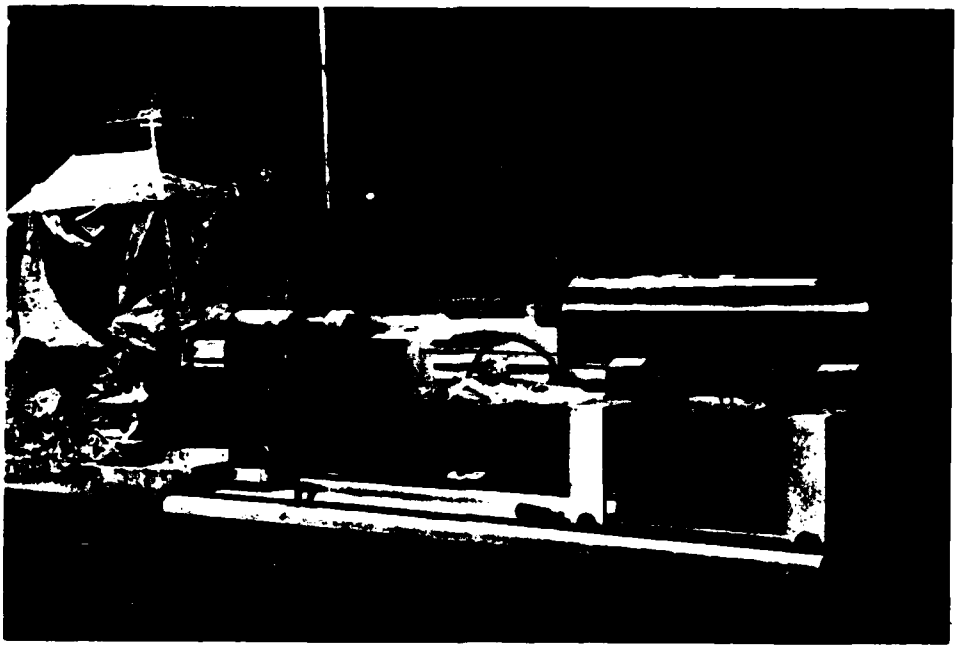

Figure 3. Reactor Tube and Rolling Furnace

leakage. These compounds are spaced to provide adequate room for maintenance work such as sealing connectors or replacing parts. The tubing was installed with minimum stress on the connections and bent in large radii to prevent pinching of the tubing conductor which could lead to leaks. The layout is designed to simplify the maze of interconnections into a pattern which can be easily traced and maintained.

The quartz reaction tube and rolling furnace assembly are shown in Figure 3. The quartz tube is securely mounted to the track by an aluminum stand which has provisions to adjust the height and direction of the quartz tube so that it fits inside the cylindrical furnace when the furnace is rolled over it. The reactor tube is held securely by the stand to reduce strain on the glass to metal seals. The track is aligned so that the rolling furnace can be positioned over the tube precisely at the same point every growth run.

An open area of the counter between the control panel and the access end of the reaction tube provides working space in which to load the source load or substrate holder into the long reaction tube. A portable exhaust hood positioned over this area catches any phosphorous smoke or other fumes that issue from the open reaction tube during maintenance and helps to maintain a net gas flow out of it. The hood is clear so that one may view work through it as necessary. All stainless steel tubing exposed to the gaseous wastes from the reactor tube in this area are covered with aluminum foil to reduce corrosion.

The use of air controlled bellows valves to simultaneously switch the hydrogen and argon prevents inadvertent hydrogen flow while the reaction tube is open. Such a mistake could lead to an explosion and

damage to the reactor. The ability to switch the PCl_3 bubbler and bypass valves off and on by a single remote valve is not only convenient for the user by eliminates strain on the glass to metal connections on the bubbler resulting from physically turning the valves in the bubbler off and on. Fewer leaks should occur as a result, and the chance of breaking the bubbler while shutting it off and on is eliminated.

In general, the reactor system is reliable and durable. Attention has been given to minimizing the presence of impurities in the system and maximizing control over the growth process. Procedures for using the system for VPE growth are discussed in the next chapter.

3. VPE GROWTH PROCEDURES

The working reactor must be charged with the appropriate reactants prior to a growth run. The first step involves loading liquid PCl_3 into the bubbler without contaminating it with oxygen. An In source is then positioned in the reaction tube, heated to 800°C for 6 hours to remove volatile impurities. After the melt is saturated with phosphorus, the reactor is ready for use. A section of InP substrate material is chemically prepared and inserted into the reactor which is then flushed with hydrogen to remove any impurities encountered during loading. The rolling furnace, which has been preheated, is rolled over the reactor tube. The PCl_3 bubbler is switched on and epitaxial growth commences after a brief melt resaturation period.

The growth of a semiconductor layer is the starting point for a wide variety of devices. Control of carrier concentration and epitaxial layer thickness is essential in the fabrication of most devices. Several growth parameters are adjusted to achieve accurate control of the process, including the temperature profile across the source and seed, PCl_3 mole fraction, various flow rates, amount of dopant, and total growth time. Purity of the PCl_3 and indium source material is essential. All these factors must be parametrically studied and adjusted until the system produces the desired epitaxial material.

3.1 START-U? AND MAINTENANCE PROCEDURES

3.1.1 Loading the PCl_3 Bubbler

The PCl_3 is loaded into the bubbler through the output PCl_3 containment valve. An ampule containing the PCl_3 is thoroughly cleaned

and placed into the transfer container which is sealed in place over the containment valve and flushed in a high argon flow. This flow in the bubbler and transfer container insures minimum contamination from atmospheric gases. The ampule is then broken and the contents poured into the bubbler. The containment valve is replaced and the transfer container removed. The H_2 flow is then reestablished.

After loading the PCl_3 into the bubbler, hydrogen is passed through it for several hours to distill off the first fraction. If this is not done, the first epitaxial layers have a higher carrier concentration than normal. A final clean up of the system to remove impurities is carried out by running the furnace 20°C hotter than a normal deposition run.

3.1.2 Melt Saturation

A fifty grams ingot of indium (Grade AlA, United Mineral and Chemical Corporation) is placed in the quartz boat and loaded into the furnace using a clean quartz transfer tube. The furnace is heated to the growth temperature and is rolled over the tube once the temperature stabilizes. The source is baked for two hours or more in a hydrogen stream to remove any impurities that entered the melt during transfer [1,2,19]. A PCl_3 flow is then introduced over the indium melt until an equilibrium phosphous concentration in the source is established.

3.1.2.1 Melt Saturation Reactions

The following reactions take place during saturation [1]. When the PCl_3 vapor enters the hot reaction tube the PCl_3 disassociates and in the presence of H_2 reacts to form P_4 (gas) and HCl (gas) with the stoichiometry:

$$4PCl_3 + 6H_2 \longrightarrow P_4 + 12HCl \quad (1)$$

With the presence of elemental indium in contact with the gas flow there occurs a reaction between the indium and P_4:

$$4In + P_4 \longrightarrow 4InP \quad (2)$$

This reaction will dominate the stochiometric composition of the gas flow by depleting P_4 from the stream until the indium is saturated with phosphorus and a solid InP crust is formed which provides a barrier between the gas stream and the indium [5].

3.1.2.2 Saturation Time

The minimum time necessary for the saturation of the melt is based on a phosphorus flux calculation [19], assuming that during saturation the phosphorus transported is completely incorporated into the melt. The minimum time for saturation of the melt is expressed by the following relation:

$$\text{Minimum time for saturation} = \frac{RT_p S(T_m)}{P(T_p)f} \times \text{moles of indium present} \quad (3)$$

where

R = ideal gas constant $\frac{\text{torr-cm}^3}{\text{mole-K}}$

T_p = temperature of PCl_3 (k)

$P(T_p)$ = equilibrium vapor pressure of PCl_3 (Torr)

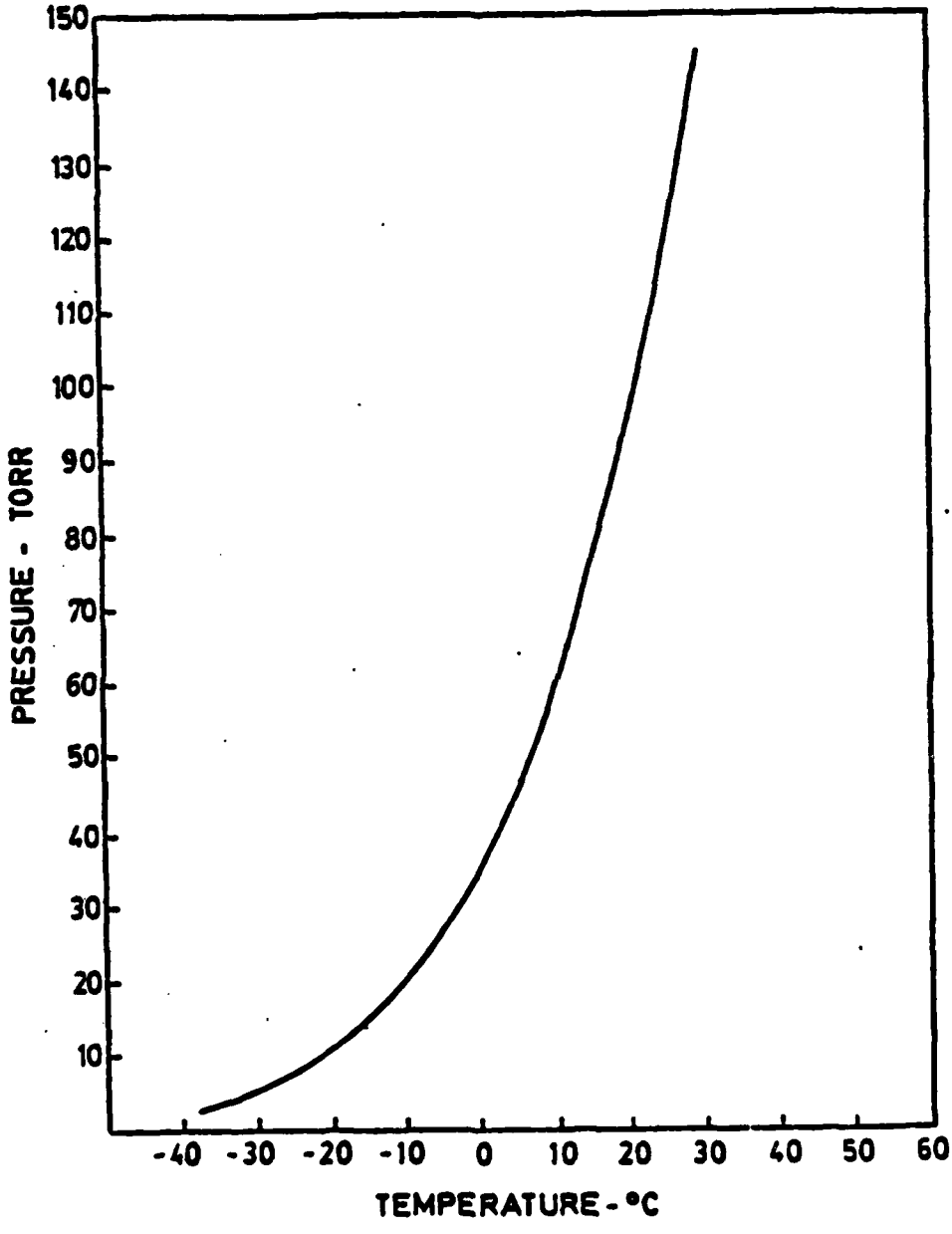

Figure 4. PCl_3 vapor pressure data.

Taken from [20]

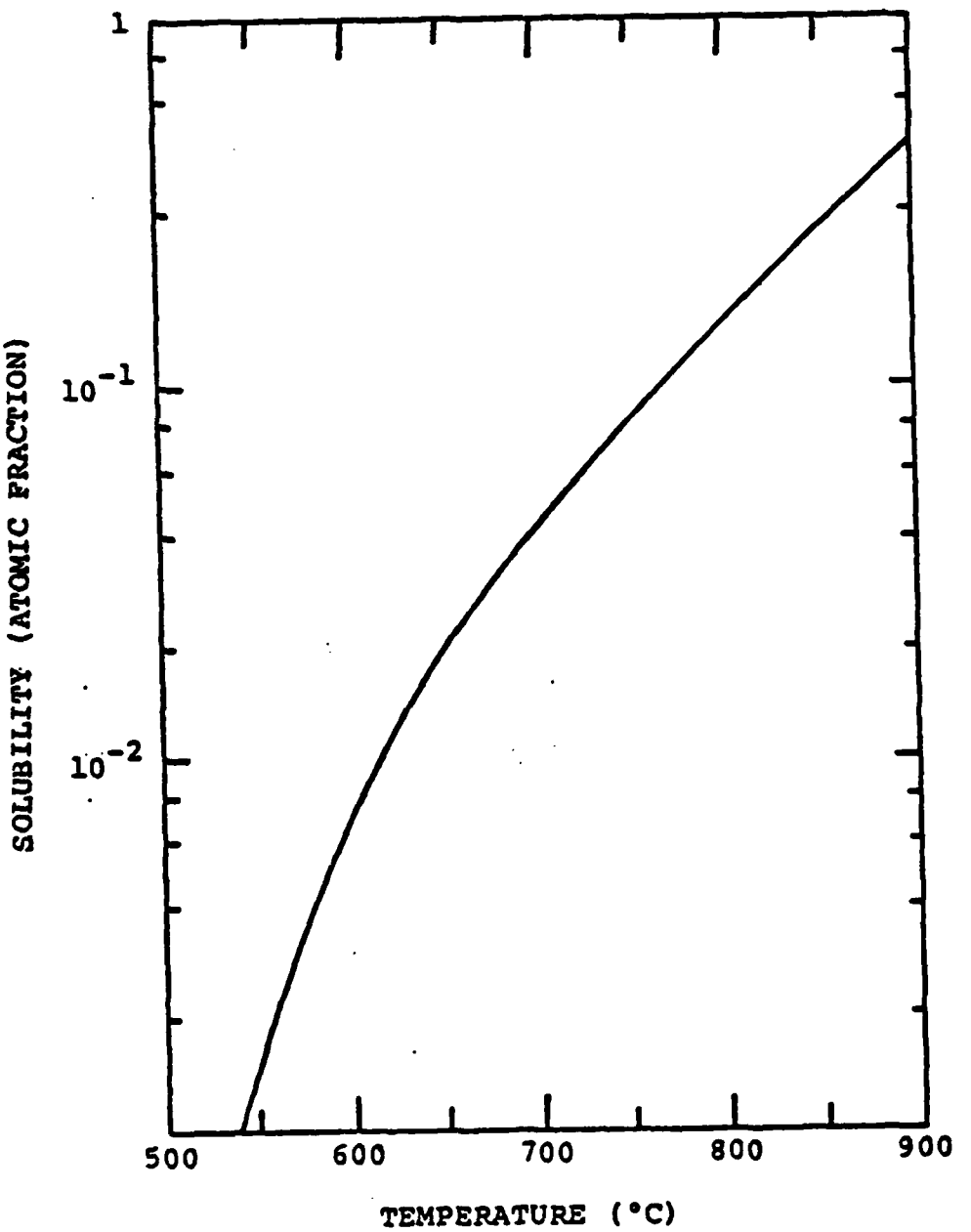

Figure 5. Solubility of InP in indium.
Taken from [21]

f = flow rate (ml/min)

$S(T_m)$ = solubility of InP in In (atomic fraction) at melt temperature T_m(K)

$P(T_p)$ is obtained from Figure 4 and $S(T_m)$ is obtained from Figure 5.

The actual values used are:

$$R = 82 \ \frac{\text{atm cm}^3}{\text{mole°K}} \times \frac{760 \text{ torr}}{\text{atm}} = 62320 \ \frac{\text{torr cm}^3}{\text{mole°K}}$$

$$T_p = 287°K \tag{2}$$

$P(T_p)$ = 73 torr; (using T_p = 14.6°C on Figure 4)

f = 100 ml/min

$S(T_m) = 6 \times 10^{-2}$

$$\text{moles of indium} = .421 = 50 \text{ g} \times \frac{1}{118.69} \frac{\text{mole}}{\text{g}}$$

Using Equation (3), the minimum time for melt saturation is 61 minutes. Note that equation (3) assumes that the total flow of H_2 is exposed to the PCl_3. To insure that equation (3) is valid the flow through the dilution is set to zero.

Actual saturation time is typically taken not less than 1.5 times greater than the minimum time to insure full saturation to account for kinetic factors which may divert some of the phosphorus away from the melt [19].

3.2 SAMPLE PREPARATION AND GROWTH PROCEDURES

3.2.1 Sample Preparation

The epitaxial layers are grown on heavily doped n-type InP. The orientation is in the 100 direction or 2° off. The substrate material is purchased from United Mineral and Chemical Corporation. Other parameters include doping density, N_d, of $1x10^{18}/cm^3$ to $2x10^{18}/cm^3$, thickness of .016 $\pm$ .001 inch, etch pit density (EPD) less than 60,000, and resistivity less than .003 ohm cm.

After the substrates are cleaved to desired dimensions, they are cleaned with organic solvents in a beaker. Trichloroethylene, acetone, and methyl alcohol in sequence are used for this purpose. The substrate is then etched in a 2% bromine-methanol solution for four minutes with mild agitation. The etch is terminated by flushing liberally with methonal. The sample is kept in methonal until just prior to insertion into the reactor to eliminate surface clouding [19]. Using this method, smooth interfaces and surfaces are obtained.

3.2.2 VPE Growth Procedures

The reactor must be flushed with argon at a high flow rate (greater than 200 cc/min) for at least 15 minutes prior to opening the reaction tube. The high flow must continue when the tube is open to minimize the penetration of atmospheric gases flowing back into the tube. This precaution is necessary to avoid contamination of the reactor and to prevent any phosphorous residue on the tube from burning with oxygen from the air.

Once the reactor is adequately purged with argon the tube is opened. The sample is removed from the methanol, dried on bibulous

paper in an N_2 flow, and immediately placed on the seed holder. The seed holder is inserted into the furnace tube to its desired position relative to the source and/or furnace temperature profile. The reactor tube is then sealed. After a few minutes the system is switched back to a hydrogen flow from the argon flow. The tube is purged with hydrogen at a flow of at least 200 cc/min for at least 30 minutes, which removes gaseous impurities on the seed, seed holder, or tube that resulted from preparation or loading the sample.

The furnace is turned on prior to sample preparation and loading. It requires approximately 1.5 hours to warm up and stabilize at the set temperatures. The furnace is preheated off the reaction tube. Once the furnace temperatures are stable and the sample has been inserted into the tube and purged in the hydrogen flow for one-half hour the furnace is rolled over the tube. After twelve minutes the furnace temperature transient has decayed and the reactor has a profile as in Figure 6.

Soon after the furnace is rolled into position the flows are set to achieve the total flow rate and PCl_3 mole fraction that are necessary to resaturate the source. The PCl_3 bubbler is turned on. After ten minutes the source is resaturated and growth begins. Flows are reset to achieve desired doping level and growth rates. The runs are typically 15 minutes to 60 minutes long depending on the current growth rate and the desired epitaxial layer thickness. The run is terminated by shutting off the bubbler, opening the bypass valve, and rolling the furnace off the tube. The quartz reaction tube and contents quench rapidly in the air.

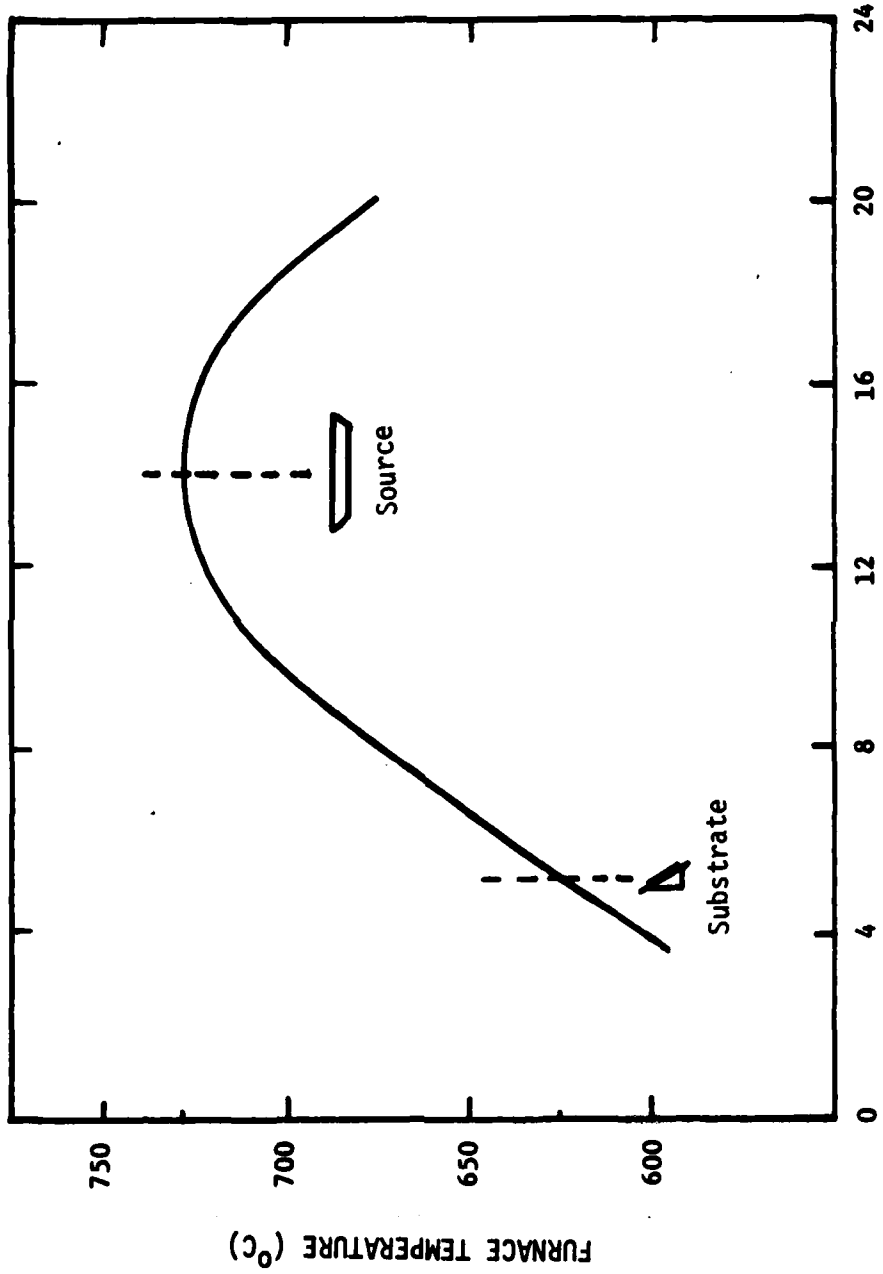

Figure 6. Temperature Profile Inside Reactor.
(Furnace is in growth position)

Before opening the reaction tube, the reactor must be purged with argon at a high flow rate for at least fifteen minutes. The tube is then opened, the extraneous crystal deposits from the run are scraped off the reactor tube wall, and the seed holder is removed from the tube. The tube is resealed and a hydrogren flow is reestablished after a short purge.

The sample, once removed from the seed holder, is then ready for evaluation.

3.2.3 Growth Reactions

Once the source is fully saturated, the fundamental reaction that is responsible for transport and deposition [1] is given by

$$4InP + 4HCl \underset{650°C}{\overset{750°C}{\rightleftharpoons}} 4InCl + P_4 + 2H_2 \qquad (4)$$

The arrow from left to right indicates the reaction of HCl with the InP crust to provide the mechanism of phosphorus and indium transport in the system. This reaction takes place at the source. The InCl, phosphorus, and hydrogen are then carried downstream toward the seed where the temperature is approximately 100°C less than the source temperature. At lower temperatures the deposition reaction (right to left) occurs to form the InP epitaxial layer. Gaseous dopants are introduced upstream from the seed but downstream from the source for incorporation into the epitaxial layer.

3.3 GROWTH PARAMETERS

The dominant growth parameters are flow rate, furnace temperature profile, and PCl_3 mole fraction. These parameters may be varied to

obtain optimal growth rates, surface conditions, and purity. Much work has been done to investigate the interdependence of the parameters and their effects on the growth process [1-7,19,22]. However, each unique reactor must still be characterized to determine its optimal set of parameters.

3.3.1 Temperature Profile Effect

The temperature profile of the reactor is given in Figure 6. The In source is normally kept at a temperature between 700°C and 750°C with the seed 100°C cooler. Our present source temperature is 700°C with seed temperature around 600°C. A 750°C source, 650°C seed temperature has also been used with no appreciable differences in physical results.

The source needs to be in a constant temperature zone to maintain the same InP saturation over the entire melt. If there are significant temperature gradients present convection and solid migration will occur. Phosphorus will be absorbed from the vapor by the source at warm points and indium phosphide will precipitate at cool points. This source inhomogeneity will decrease the mole fraction of PCl_3 at the seed which increases the impurity concentration of the grown layer [22]. Thus a significant temperature gradient across the source increases the impurity concentration in a manner that is difficult to control. To avoid significant source gradient effects the source must have a gradient $\leq$ 0.1°C/cm [44]. Refer to Appendix 8.3 for a more detailed discussion.

3.3.2 Mole Fraction Effect

The mole fraction trends in the PCl_3-In-H_2 process are well known. In general, the growth rate increases with an increase in mole fraction while the net doping increases with decreasing mole fraction [1,4]. Small changes in PCl_3 mole fraction is important.

The mole fraction of PCl_3 in the hydrogen carrier is dependent upon the temperature of the PCl_3 liquid in the bubbler and the amount of H_2 dilution downstream. Both are controllable in our system.

The mole fraction of PCl_3 in the vapor from the bubbler is calculated as the partial pressure of the PCl_3 divided by the total vapor pressure of the PCl_3 and H_2. This is expressed by:

$$\text{mole fraction } PCl_3 = \frac{P_p}{P_p + P_H} \tag{5}$$

where

P_p = equilibrium partial pressure of PCl_3 (torr)

P_H = equilibrium partial pressure of PCl_3 (torr)

The partial pressure of PCl_3 at a given temperature may be obtained graphically from Figure 4 or analytically from the expression [23].

$$\log_{10} P = (-.2185A/T) + B \tag{6}$$

where A = molar heat of vaporization of PCl_3 = 7997.0

B = 7.925795

T = temperature of PCl_3 in °K

P = partial pressure of PCl_3

The denominator of Equation (5) is the total vapor pressure; usually 760 torr. If T = 14.6°C the PCl_3 mole fraction is 9.3 percent.

The mole fraction of PCl_3 in the hydrogen flow is further reduced by dilution. A schematic of the dilution system is given in Figure 7. A pure H_2 flow, f_2, is mixed with the PCl_3/H_2 mixture, f_1, to give a new mole fraction for the gas flow f_3 given by:

$$MF_3 = (MF_1)\frac{f_1}{f_1+f_2} = \frac{(MF_1)}{1+(f_2/f_1)} \qquad (7)$$

where

MF_3 = mole fraction of PCl_3 in flow f_3;

MF_1 = mole fraction of PCl_3 in flow f_1

f_2, f_1 are flow rates in cc/min

Equations (5-7) reveal that the final mole fraction is a function of the original mole fraction which is a function of temperature and the ratio of the dilution flow over the original flow. Figure 8 shows the effect of changing PCl_3 temperature and dilution on the resultant mole fraction. If the PCl_3 temperature is held constant, the mole fraction becomes a function of dilution only. Table 1 gives specific

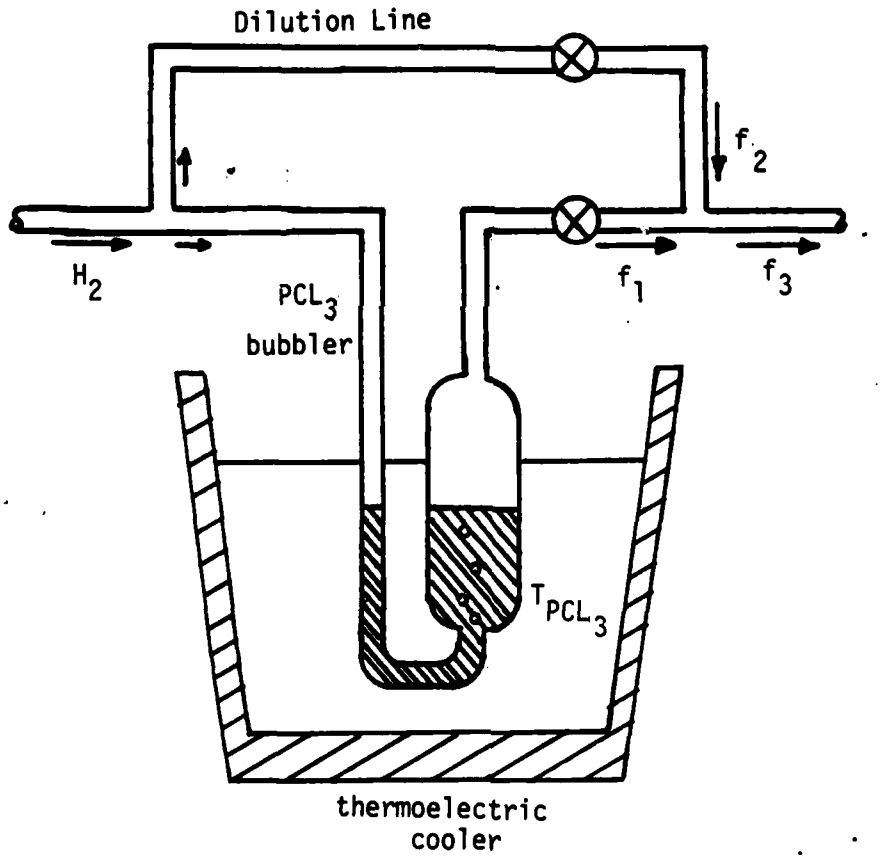

Figure 7: Schematic of system for control of PCL_3 mole fraction

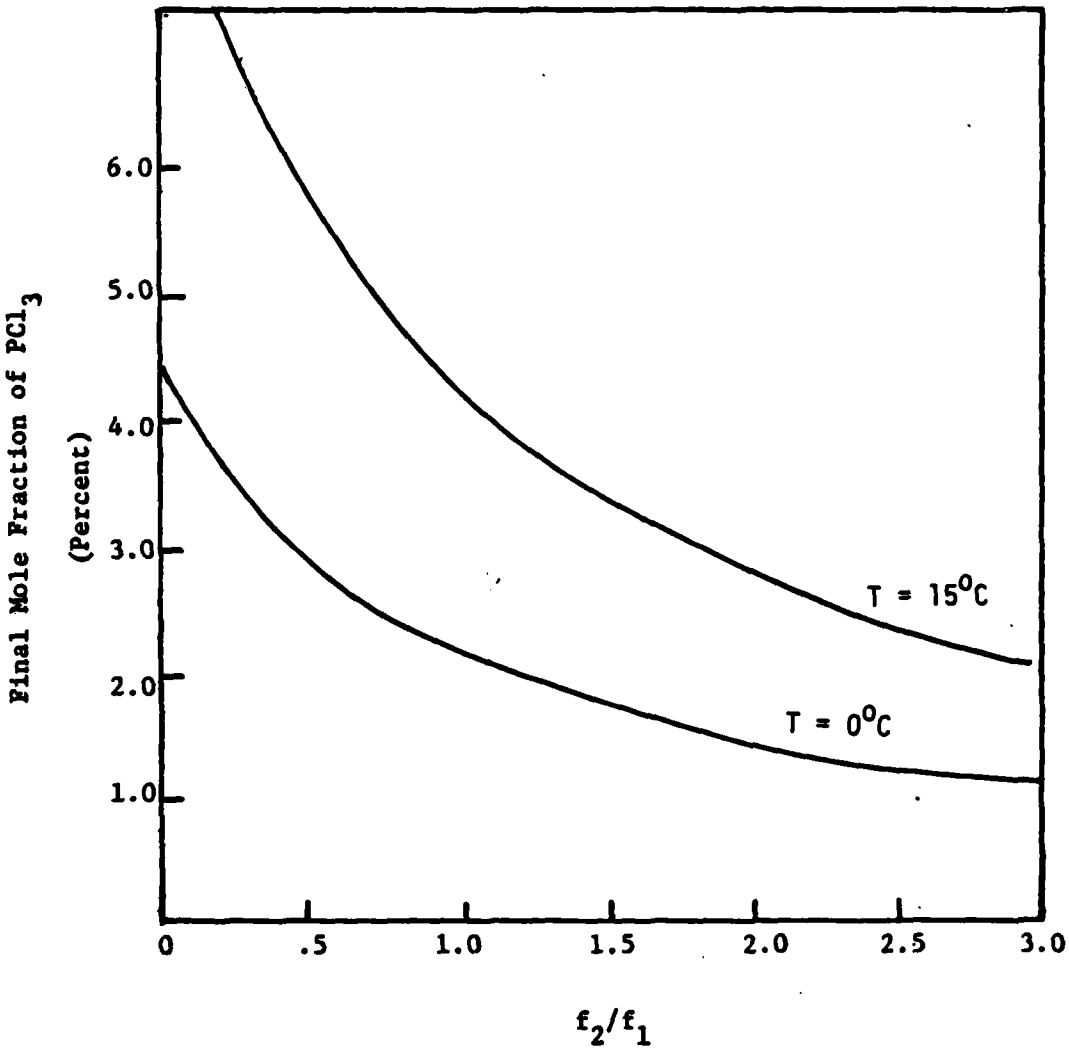

Figure 8. Final Mole Fraction as a Function of Dilution and PCl_3 Temperature

Table 1

Mole Fraction of PCl_3 vs Dilution

$T_{PCl_3} = 14.6°C$

f_2/f_1	% Mole Fraction of PCl_3 in flow f_3
0	8.5
.50	5.7
1.0	4.2
1.25	3.8
1.50	3.4
1.75	3.0
2.00	2.8
2.25	2.6
2.50	2.4
2.75	2.3
3.0	2.1

mole fractions for various dilution ratios with a constant PCl_3 temperature. Note that the maximum final mole fraction is limited by the original mole fraction.

The mole fraction of PCl_3 at the seed is further influenced by reactions at the source and by the dilution of the dopant line. The mole fraction influence by the source occurs when the source is not adequately saturated and absorbs phosphorus from the flow [22]. The dopant line flow further dilutes and decreases the mole fraction of PCl_3 at the seed. If the doping concentration is a function of mole fraction at the substrate, as some workers have proposed [6,24], then it is helpful to keep the dopant line flow small compared to the main flow.

3.3.3 Flow Rate

Although the flow rate has some effect on growth rate and impurity concentrations, these effects are secondary to mole fraction and profile effects [25]. Higher flows ($\geq$ 100 ml/min) do appear to give better surfaces than low flows, however.

The goal of this VPE growth is the creation of semiconductor material suitable for device fabrication. The grown layer should have a smooth surface and a low defect smooth interface at the substrate. The thickness should be controllable and uniform across the sample. Electrically, the material should have a specific carrier concentration profile with depth and exhibit high electron mobility. After a sample is grown, the surface is inspected optically. Next a small section is cleaved off and etched to delineate the interface and hence reveal the epitaxial layer thickness. The doping profile is obtained by fabricating

a Schottky diode on the surface and making capacitance-voltage measurements.

The results of the evaluation serve a dual role. They become a basis on which to modify the growth parameters for subsequent grow runs and are also needed in designing and fabricating devices from the grown material. Therefore the ability to evaluate material and fabricate a device from it are important factors in crystal growth technology.

4. SCHOTTKY-BARRIERS ON InP

4.1 INTRODUCTION

Capacitance-voltage measurements are employed to evaluate the carrier concentration profile of an epitaxial layer of InP grown on an n^{++} substrate. This process involves fabricating a Schottky-barrier on the surface, measuring the C-V curve when the diode is reverse biased, and calculating the doping concentration from that curve. If the reverse saturation current of the rectifying contact is too large the C-V measurements will not be accurate. Therefore Schottky diodes with low reverse leakage currents are essential for correct evaluation of the carrier concentration versus depth in an epitaxial layer.

Rectifying metal/InP junctions are also used in a wide variety of devices including Gunn oscillators and field effect transistors. The structure desired for the velocity - electric field characterization of InP also requires a Schottky contact. Since metal junctions are an important part of many devices, successful junction fabrication techniques are necessary from both material evaluation and device fabrication perspectives.

Unfortunately, Schottky diodes with high barrier heights (and low reverse leakage current) are difficult to fabricate with InP. The traditional procedure of evaporating aluminum or other metals directly down onto an InP surface results in junctions with very low barrier heights (.2 or .3eV) that act almost ohmic. In addition, the barrier height of such a junction does not depend on the work function of the metal as traditional contact theory predicts.

It will be shown that the unusual behavior of these metal/InP contacts can be attributed to chemical reactions between the metal electrode and the semiconductor which degrade the junction and to the high surface state density of InP which clamps the Fermi level in the semiconductor regardless of the metal. The problem may be avoided by inserting a thin layer of oxide between the metal and the semiconductor. The thickness of this interfacial layer may be changed in order to alter the junction's effective barrier height, but must be thin enough to retain Schottky device characteristics. Techniques for formation of such an interfacial layer, including chemical etches and heat treatments, will also be discussed.

4.2 TRADITIONAL METAL-SEMICONDUCTOR MODEL

The traditional theory of metal-semiconductor contacts [12] assumes that the barrier height of the junction depends primarily on the difference between the work function of the metal, ϕ_m, and that of the semiconductor ϕ_s. The work function is defined as the energy difference between the vacuum level and the Fermi level. The energy level diagram of a metal/n-type semiconductor contact with $\phi_m > \phi_s$ is shown in Figure 9 [25]. Before the contact (Figure 9a) the Fermi level is above that of the metal by an amount $\phi_m - \phi_s$. After contact (Figure 9b), an exchange of charge occurs which lowers the energy level in the bulk semiconductor until the Fermi levels in both materials are equal. Electrons from the surface layer of the semiconductor flow into the metal, leaving ionized donors behind in the surface layer [Figure 9]. The height of the barrier, ϕ_B, is now proportional to the quantity $(\phi_m - \phi_s)$.

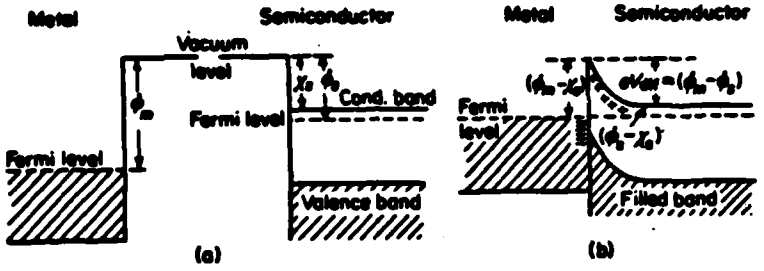

Energy-level diagram of a metal *n*-type semiconductor contact with $\phi_m > \phi_s$, where ϕ_m and ϕ_s are the work functions of metal and semiconductor, respectively. (a) Energy-level diagram before contact. (b) Energy-level diagram after contact. The Fermi level is now at equal height; V_{diff} is the diffusion potential.

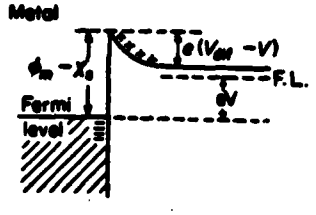

(c) To show that the metal-semiconductor contact is rectifying. V_{diff} is the diffusion potential. A voltage $-V$ is applied to the semiconductor. The Fermi level in the bulk semiconductor has shifted by an amount eV.

Figure 9: Energy level diagrams for rectifying contacts. Taken from [25].

Due to thermal agitation, some of the electrons in the metal will have enough energy to cross the potential barrier into the semiconductor and, due to diffusion, some electrons in the semiconductor cross the potential barrier into the metal. In equilibrium this gives rise to equal and opposite currents I_s crossing the barrier.

If a voltage-V is applied to the semiconductor, as in Figure 9c, the barrier for electrons going from left to right has not changed, and hence the corresponding current from right to left has not changed either. But since the energy levels in the conduction band have been raised by an amount eV, the barrier for electrons going from right to left has been lowered by an amount eV; as a consequence the corresponding current from left to right has changed by a factor exp (eV/kT). Consequently, the I-V characteristic is given by:

$$I = AJs \left[\exp \left(\frac{eV}{kT}\right) - 1\right] \tag{13}$$

Simple thermionic emission theory predicts that the saturation current density is given by [25]:

$$J_s = A^* T^2 \exp \left[\frac{-q\phi_B}{kT}\right] \tag{14}$$

These equations show that the barrier height plays an important role in determining the diode characteristics, especially the reverse saturation current.

Elementary metal-semiconductor theory predicts that the barrier height ϕ_B of a metal-(n type) semiconductor junction will decrease if

metals with lower work functions are used. Eventually, when $\phi_m \sim \phi_s$, the junction becomes ohmic. The energy band diagrams for such a case is shown in Figure 10 [25]. In this case, electrons flow from the metal into the semiconductor, thus increasing the Fermi level in the bulk semiconductor. Since there is no space charge layer in the rectifying contact, an applied voltage is merely distributed across the bulk semiconductor. The effect of an applied bias is shown in Figures 10c and 10d.

According to traditional contact theory, comparison of the work functions of the metal and semiconductor will indicate whether the junction should be ohmic or rectifying. For n type semiconductor $\phi_m > \phi_s$ should result in a rectifying contact, and $\phi_m \sim \phi_s$ in an ohmic contact. For rectifying contacts the largest value of ϕ_m should give the smallest saturation current, I_s.

4.3 EFFECT OF SURFACE STATES

Although the simple theory of metal-semiconductor contacts predicts that the work function should be the dominant parameter in controlling the barrier height, these predictions break down if there is a high density of surface states present. Surface states, if present in the energy gap, have the property of pinning the Fermi level at the surface [16] regardless of the work function of the metal. An energy level diagram of an n-type semiconductor with surface states is shown in Figure 11 [25]. In a vacuum, electrons from the surface layer of the semiconductor fill the surface states, leaving behind a distributed positive charge due to the ionized donors. This rearrangement of charge lowers the Fermi level in the bulk semiconductor and creates a

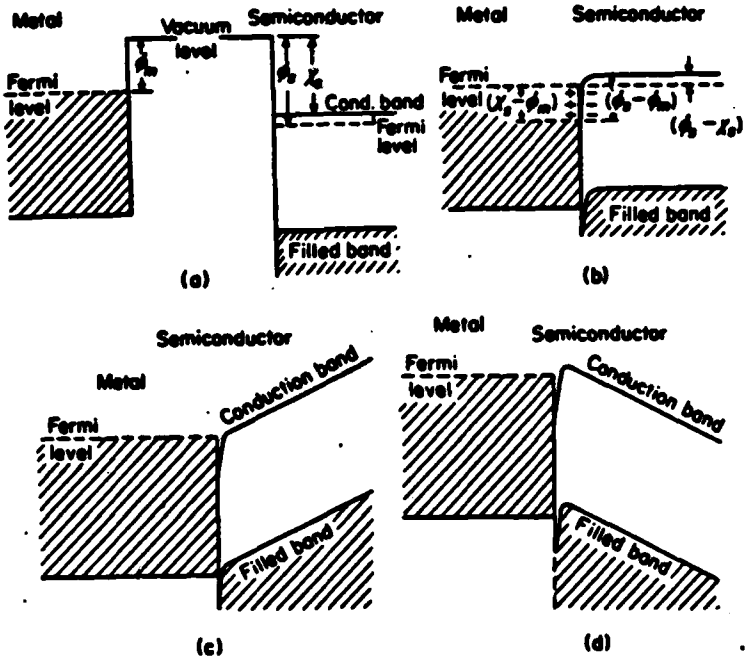

Energy-level diagram of a metal *n*-type semiconductor contact with $\phi_m < \phi_s$, where ϕ_m and ϕ_s are the work functions of metal and semiconductor, respectively. (a) Energy-level diagram before contact. (b) Energy-level diagram after contact. This contact is ohmic. (c) A negative voltage is applied to the contact. (d) A positive voltage is applied to the contact.

Figure 10: Energy level diagrams for ohmic contacts.

Taken from [25].

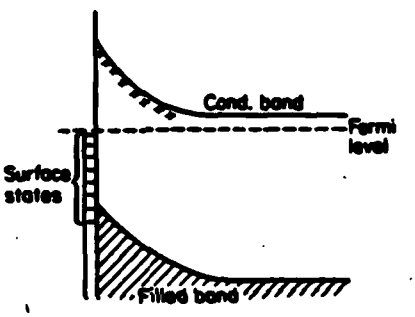

Energy-level diagram of an n-type semiconductor with surface states. The filled surface states may make a metal-semiconductor contact rectifying even if the condition $\phi_m > \phi_s$ is not satisfied.

Figure 11: Effect of surface states

Taken from [25]

natural surface barrier. This effectively pins the Fermi level at the surface.

Contacting such a semiconductor to metal allows some of the electrons in the surface states to flow into the metal, but doesn't alter the charge in the surface layer significantly. Making contact to metals of different work functions then means that a different portion of the occupied states are emptied into the metal. Since this does not change the space charge at the barrier, the barrier height remains constant.

4.4 NATURE OF METAL/InP INTERFACE

The electrical properties of indium phosphide-metal contact are generally insensitive to work function. The dependence is illustrated by a plot of barrier height vs. work function in Figure 12 [11]. In this study Schottky barriers were formed between atomically clean surfaces of InP and a range of metals deposited by evaporation in an ultrahigh vacuum. Also shown are barriers formed on (110) InP etched in bromine-methonal and thus having a thin oxide layer between the semiconductor and the metal. For the atomically clean surfaces, there appears to be no simple dependence of ϕ_B on metal work function; Al, Fe, and Ni form very low barrier heights where as Ag, Cu, and Au form barrier heights around 0.5 eV. For the etched surfaces ϕ_B is largely independent of the metal work function and appears to be pinned around 0.5 eV.

A high density of surface states appears to be the primary mechanism which clamps the barrier height in etched InP/metal contacts. Although no intrinsic surface states are found in the band gap of

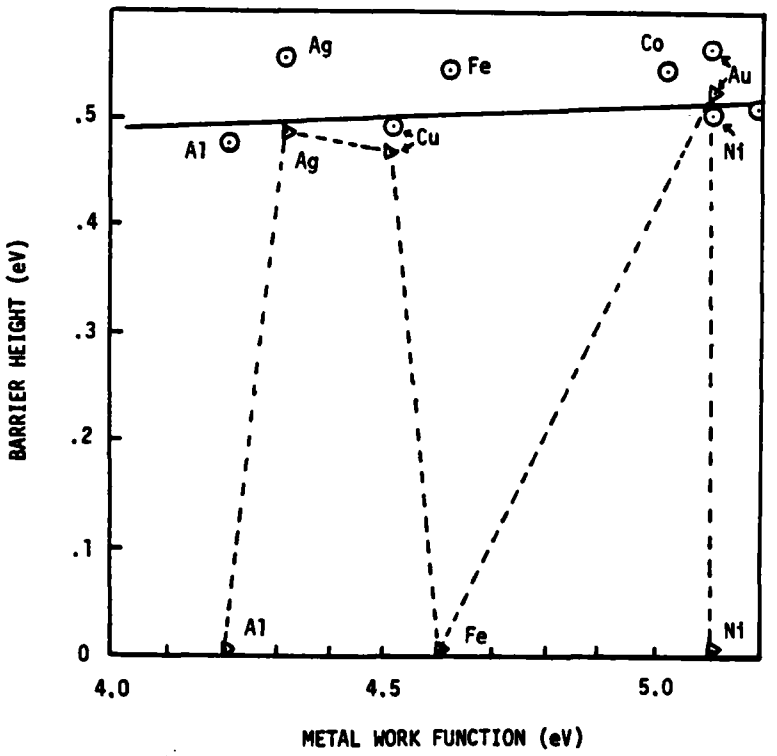

Figure 12: Plot of Schottky barrier height against the work function of the metal electrode for:

a) atomically clean (110) InP surfaces (▷)

b) etched (110) InP faces (⊙)

Taken from [11]

atomically clean InP in a vacuum [16], defects formed by the addition of oxygen on to InP result in extrinsic surface states which clamp the Fermi level. Spicer and others [27] have found that less than a monolayer of oxygen is necessary for this pinning to occur and that once the defects are formed at the interface further layers of oxygen have little effect on the Fermi level. Thus impurity and defect interactions at the interface play a dominant role in clamping the barrier height of etched InP contacts.

4.5 CHEMICAL EFFECTS ON ATOMICALLY CLEAN InP/METAL CONTACTS

The behavior of metal contacts on atomically clean InP is more complicated than that of etched contacts, since the barrier heights are not all pinned at the same level. The fact that the barrier heights for Au, Ag and Cu contacts are all clamped to the same level as for etched contacts suggests that these metals are forming defects and extrinsic states which clamp the Fermi level in a manner similar to oxygen. This effect was observed and verified by Spicer [27]. However, the ohmic behavior of the Al, Ni, and Fe contacts cannot be explained by this theory. Other effects must be considered.

There are indications that the interface of atomically clean InP surfaces and metals is dominated by chemical effects. Table 2 [11] lists the heats of reaction for the most stable compounds that Au, Ag, Cu, In, Al, and Fe form with phosphorus. Figure 13 [11] combines the data on barrier height versus metal in Figure 12 with the heat of reactions of the metal electrodes with phosphorus given in Table 2. From Figure 13 and Table 2 it is clear that one obtains ohmic contact behavior for metals such as Al or Ni which are substantially more

TABLE 2

Heats of Reaction

(Metal + InP → metal phosphide + In)

Most stable compound	Au_2P_3	A_gP_2	CuP_2	InP	AlP	Fe_3P	Nl_5P_2
Heat of reaction (eV/metal atom)	+1.73	+1.37	+.46	0	0.81	-0.82	-0.31

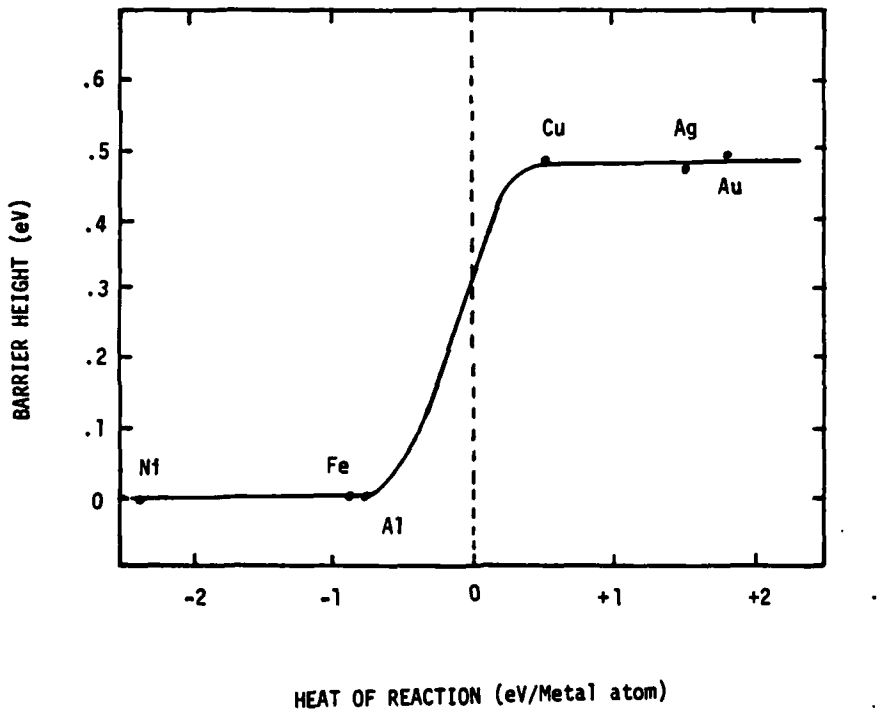

Figure 13. Plot of Schottky-barrier height as a function of heat of reaction of the metal electrode with phosphorous as outlined in Table 2.

stable than InP. On the other hand, for less active metals such as silver or gold, Schottky-barriers are observed. Chemical effects therefore appear to be significant for Schottky-barriers of metal on atomically clean surfaces. The barrier height for Schottky diodes with an interfacial oxide layer is immune from these chemical effects since the oxide layer prevents the phosphorus from reacting with the metal. Hence the barrier height for the "etched" faces remain constant with choice of metal as in Figure 12(b).

4.6 EFFECT OF INTERFACIAL OXIDE LAYER

A thin layer of oxide prevents the chemical reactions which occur between reactive metals [15] and ultra clean InP and allows Schottky-barriers to be formed with barrier heights around 0.5 eV [16]. This barrier height is about the same as that obtained for unreactive metals such as Au and Ag on clean surfaces. Several researchers have studied the effect of the oxide layers on the properties of InP/metal Schottky barriers [7-16]. A thin layer (6nm) appears to to have little effect on the characteristics of the diode other than increasing the effective barrier height, ϕ_B, given by [12]:

$$\phi'_B = \phi_B + D\,d \qquad (15)$$

where: ϕ_B = actual barrier height determined (directly) by photoelectric response

d = oxide layer thickness

D = experimental coefficient of increase of barrier height with thickness d.

The oxide layer decreases the saturation current of the diode and thus increases the effective barrier height as determined from C-V or I-V data. The effective barrier height increases linearly with the oxide thickness, d, as shown by Equation 15. Values of D for GaAs, InP and Si are seen to range from 0.5×10^6 to $1.75 \times 10^6 Vcm^{-1}$ [12].

Although equation 15 implies that a large increase in ϕ_B' with d is possible, the layer thickness is bound by practical considerations. As d is increased a greater part of the terminal voltage is dropped across the oxide, causing the ideality factor n of the diode to increase. As the ideality factor increases the I-V characteristics of the device flatten out and tend toward ohmic behavior [13]. Also the series capacitance of the oxide film will decrease as the oxide film thickness increases. Eventually the capacitance of the oxide will be small enough to introduce significant error into the C-V measurements, as the capacitance that the meter reads becomes much smaller than the actual barrier capacitance.

The following conditions [12] must apply if interfacial layers are to be used for improving the quality of Schottky-barriers:

1) The oxide should be as thin as possible, to minimize the increase in the ideality factor n of the diode. Since $\phi_B' = \phi_B + D\ d$, for a given increase in effective barrier height D must be as large as possible. This in turn means that an oxide with a small value of electron affinity X_{ox} must be used.

2) The oxide should not contain a residual space charge which will vary the shape and effective height of the barrier unpredictably.

3) The oxide should not contain deep trapping levels which would assist the tunneling process and hence decrease D.

4) The interfacial layer should not degrade the diode reverse characteristics.

5) The insulating layer need not be the natural oxide. Any good insulator satisfying the above conditions will suffice.

Oxide layers have been used by many workers to successfully create reproducible Schottky diodes on InP with Au, Al and Au metalizations [1,10,13,14,16]. One reported method is to etch the sample in 2% bromine methonal just prior to evaporation of the metal contact [10,14]. The etch deposits a very thin indium oxide layer that serves as an effective interfacial layer. An etch in "aurostrip" also serves the same purpose. Methods of achieving more controllable oxide layers include low temperature plasma oxidation [15] or more complicated deposition techniques [13].

4.7 HEAT TREATMENTS

Significant improvement of InP Schottky diode characteristics can be obtained by heat treatment prior to, during and after evaporation. Morgan, Howles, and Delvin report that heating the surfaces in a vacuum to 250°C before evaporation and maintaining them at 150°C during it produces Au/n-InP devices that are significantly more reproducible and electrically self consistent than unheated devices [10]. Roberts and Pande obtained reproducible Au/InP contacts by adding 1% weight of

titanium to the gold and alloying this mixture at a vacuum of 10^{-5} torr before evaporation. Following evaporation, the samples were annealled at 250°C for two minutes at a pressure of 10^{-4} torr [14]. In both cases, the samples were pre-etched in a 2% bromine-methonal solution to provide an interfacial oxide layer. Both groups found that the barrier height as measured by photoelectric response was 0.53 eV for their Au/InP contacts.

Heat treatments have also been used on Al/InP Schottky diodes successfully. Christou and Anderson [13] found that sintering Al/InP diodes in a 10^{4} torr vacuum at 250°C for 4 hours or at 1 atmosphere at 250°C for 30 minutes significantly increased the barrier height; (0.25 eV to 0.55 eV for air sintering). The barrier height increases are due to oxygen build-up at the interface. Sintering redistributes the oxygen throughout the Al film, and in the case of the 250°C anneal, results in a pile-up of oxygen at the interface and at the front surface in the form of P_2O_5. Auger electron spectroscopy studies of the metal-semiconductor interface indicate an excellent correlation between barrier height increases and oxygen build-up at the Al/InP interface [13].

Heating the surface in a vacuum serves to desorb the surface of interfacial layers. Christou and Anderson used 300°C for 15 minutes in 1×10^{-9} torr vacuum [9]. Morgan, Holwes, and Delvin [10] used 250°C in a vacuum citing studies on GaAs and InP [27,28] showing that 250°C was the minimum temperature required to remove the majority of loosely bonded surface contaminants. In their study of sintering [13], Christou and Anderson did not see a significant increase in barrier height from

vacuum desorbing the InP surface of interfacial oxides prior to metalization. However, it did create enough of an increase in barrier height to merit using desorption methods in later work [10].

On etched (110) substrates, Williams [16] reports a decrease in barrier height for Au and Ag with annealling. For Al, the barrier height slightly increased, up to about 200%, then decreased for higher anneal temperatures. The annealled Al contact was more stable than the annealled Au or Ag contacts. At first glance this decrease in barrier height with annealling seems to contradict the findings of others (Christou, Morgan, Roberts). However, the (110) orientation of substrate has a much higher rate of diffusion for the metals compared to the (100) orientation, thus interdiffusion of Au or Ag into the InP is significantly more of a problem for the (110) orientation than for (100). Hence Williams' results for temperature dependence of (110) surfaces are not applicable to (100) surfaces.

Annealling at temperatures around 250°C is helpful in diffusing oxide to the interface and creating P_2O_5 or InO_5 there without other major diffusion effects. Higher temperatures bring more drastic diffusion effects which tend to degrade the junction. Clarke [1] notes that the congruent evaporating temperature for InP is 360°C and at temperatures in excess of this the vapor pressure of phosphorus over the crystal rises rapidly causing phosphorus loss and an indium rich wafer surface. Above 400°C interdiffusion of Au or Ag into the semiconductor becomes significant, even with an interfacial layer [16]. Aluminum is more stable at higher temperatures, primarily because the formation of Al_2O_3 at the interface prevents worse diffusion.

4.8 SUMMARY

Based on the results of Morgan, Williams, and others [7-16] we have chosen to fabricate MIS Schottky contacts on InP by etching the sample just prior to the metal deposition. Sintering was also employed to increase the effective barrier height of aluminum contacts. Using these methods, Schottky-barriers suitable for C-V measurements were obtained. The particular processes and results are described in the next chapter.

5. RESULTS AND EVALUATIONS

The reactor system and growth techniques described in previous chapters have been employed to grow several samples of epitaxial InP. After each growth run the layer thickness, surface quality, electrical character, and other properties of the epitaxial material were evaluated. The evaluations are divided into two categories: physical and electrical. The former includes those properties which can be observed optically like surface quality and epitaxy thickness. The latter category involves determining the net carrier concentration profile with depth in the material. From these results one can calculate the growth rate, impurity concentration, and other parameters useful for crystal growth and device fabrication.

This chapter is organized in three parts. The first one covers the techniques used to evaluate the epitaxial material. The second section deals with the results of the physical evaluations and the third with those of the electrical evaluation. This last section is divided into two parts because C-V doping profiles measurement require the successful fabrication of Schottky diodes which is a nontrivial task on InP. Electrical properties include both InP/metal contacts and doping profiles.

5.1 SAMPLE EVALUATION TECHNIQUES

5.1.1 Physical Properties

Evaluation of the physical characteristics of the grown layers consists of analysis of surface morphology, measurement of layer thickness, and characterizing salient features of the delineated

interface (interfacial irregularities, signs of poor surface preparation crystal strain propagation through the interface, etc.)

The as grown samples are taken and subjected to microscopic examination of the surface of the epitaxial layer. Small laminae of the surface are cleaved (on the back side of sample) and the interfaces of each laminate are made visible with the use of a delineation etch [19]. It consists of immersion of the cleaved sections of the samples for 40 seconds in a solution of equal volumes of A and B where

$$A = 60gKOH + 250\ ml\ H_2O \tag{8}$$

$$B = 40gK_3Fe(CN)_6 + 250\ ml\ H_2O \tag{9}$$

The cleaved sections are rinsed in DI water and dried with bibulous paper in an N_2 flow. Measurement of the layer's thickness is then determined optically while simultaneously determining interfacial characteristics.

5.1.2 Electrical Properties

Doping profiles are obtained using capacitance voltage measurements. This involves evaporating a number of 20 mil diameter aluminum Schottky-barrier dots on the epitaxial layer. The dot is biased negative with respect to the substrate and the capacitance of the depleted region under the dot is measured as a function of the applied bias. From this data the doping concentration profile can be calculated. It is given by

$$n(X) = \frac{-C^3}{q\,A^3\left(\frac{dC}{dV}\right)} \tag{10}$$

$$X = \frac{\varepsilon A}{C} \tag{11}$$

where

C = depletion capacitance

V = applied bias to dot

A = dot area

X = depletion distance into the epitaxy

The range of x over which the carrier concentration can be accurately measured is primarily limited by the amount of leakage current in the Schottky-barrier. Most C-V meters measure the capacitance via phase shifts of a 1 MHz signal. A shunt or series resistance added to the depletion capacitance changes the phase shift so that the meter reading is not the real depletion capacitance. High leakage current indicates a low shunt resistance in the diode which degrades the accuracy of the measurement. Therefore the I-V characteristics of each Schottky diode are inspected before C-V measurements are taken.

A sample with several diodes is placed in a probe station which can be connected to either a curve tracer or a C-V meter. One of the diodes is probed and its I-V characteristics measured. If the reverse leakage is low enough for accurate C-V measurements the probe is switched to the C-V meter and a doping profile obtained. Otherwise that diode is rejected and another probed. If no diodes on the

samples can be used for C-V measurements, the metalization is etched off and a new set of diodes are fabricated on the sample. This process continues until a diode with low leakage is obtained.

5.2 RESULTS OF PHYSICAL EVALUATIONS

The first set of runs were performed to determine how the physical properties of the layers depended on system parameters. The results are summarized in Tables 3 and 4. No significant effects on surface quality or growth rates from changing the source temperature from 750°C to 700°C were found. Drawing on the work of Green [19] who found that growth at lower temperatures reduces impurity incorporation, the source was maintained at 705°C and the seed at 620°C for most of the runs. Use of these temperatures resulted in adequate growth rates and fairly good surface quality. Initial difficulties with C-V measurements on the n^+ substrates precluded accurately assessing the effect of temperature on purity.

The growth rate seems to be controlled primarily by the depletion of the source. Figure 14 presents the growth rate as a function of the source run number. It drops from a high of 25 μm/hr for the first run to zero for the seventh run. It levels off slightly for the second, third, and fourth run, averaging about 18 μm/hr before dropping off significantly for later runs. The second source followed a similar pattern with the exception of the second run.

The flow rate was kept at 150 ml/min. This value was chosen because it's moderate level gave good results in terms of surface and growth rates. Reducing the flow to 60 ml/min resulted in poor surface quality.

TABLE 3

VPE Growth Parameters and Results (1st melt)

Parameters					Results		
Sample #	flow rate (ml/min)	source temp. (°C)	substrate temp. (°C)	mole PCl_3 fraction (%)	layer thickness (μm)	surface quality	growth rate (μm/hr)
1	150	650	750	3.0	33	fair	25
2	150	620	705	2.3	1	good	20
3	150	620	705	2.3	6	fair	18
4	60	620	705	2.3	8	poor	16
5	150	620	705	4.2	3	shiny	7
6	150	620	705	2.3	1	shiny	2
7	150	620	705	2.5	0	fair	0

TABLE 4

VPE Growth Parameters and Results (2nd melt)

Parameters					Results		
Sample #	flow rate (ml/min)	source temp. (°C)	substrate temp. (°C)	PCl_3 mole fraction (%)	layer thickness (μm)	surface quality	growth rate (μm/hr)
8	150	725	630	2.3	7	fair	25
9	150	705	625	2.3	4	good	12
10	150	705	625	2.3	6	shiny	18
11	150	705	625	2.3	5	good	14

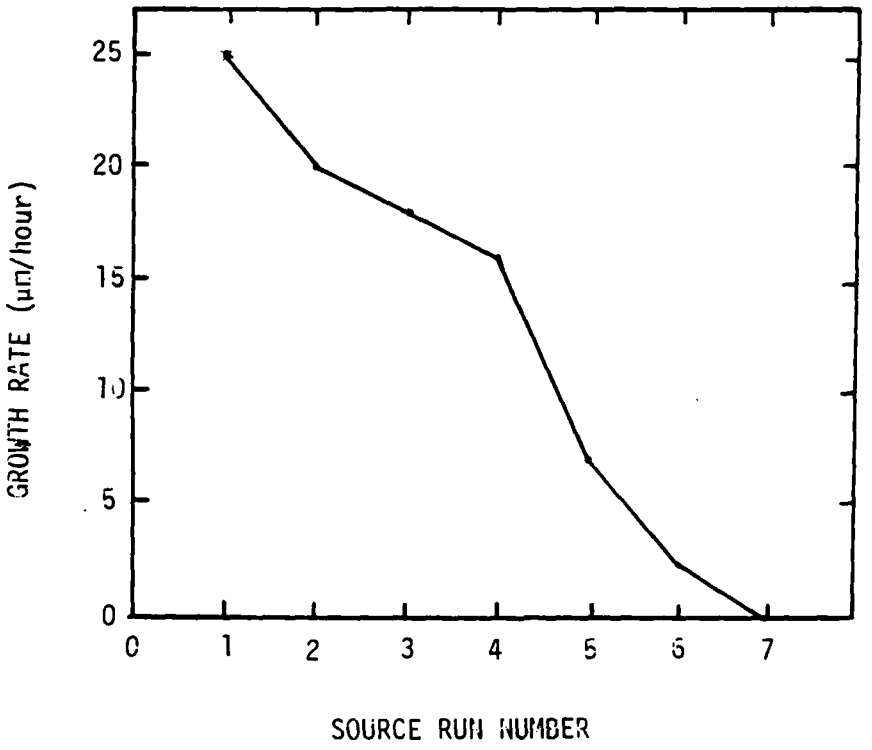

Figure 14: Growth rate as a function of source depletion

Figure 15 shows a magnified view of an layer etched in A-B. The interfaces were usually smooth and the layer thickness relatively uniform over the entire sample. Figure 16 shows a typical surface. They are normally fairly shiny. The quality of the surface was not always uniform over the sample, due to kinetic effects at the substrate.

The mole fraction at the source was calculated to be 2.3%, in the 1 to 4% range that most workers have reported success [2,4,19]. The particular effect of PCL_3 mole fraction at the source for this particular system still needs to be found. However, the literature predicts that an increase in mole fraction will decrease the impurity incorporated into the layer [4].

The effects of temperature variation across the source include a loss in control of PCl_3 mole fraction and rapid depletion of the melt. [See Appendix 8.3]. Methods employed to reduce this temperature variation, which presently is within $\pm$ 5°C over the source, include changing the set points on the two furnace zones, using a shortened source boat and placing resistors in parallel with the furnace windings. Further tuning of the reactor to achieve a longer flat zone is recommended. Currently the flat region ($\pm$ 0.5°C) is about two inches long with a source boat of the same length. This leaves too little room for error in placing the source exactly in the flat zone of the rolling furnace.

At present the standard growth parameters of 2.3% PCl_3 mole fraction, 150 ml/min flow rate, and 705°C source with 620°C substrate seem to yield epitaxial layers with good surfaces, uniform thicknesses,

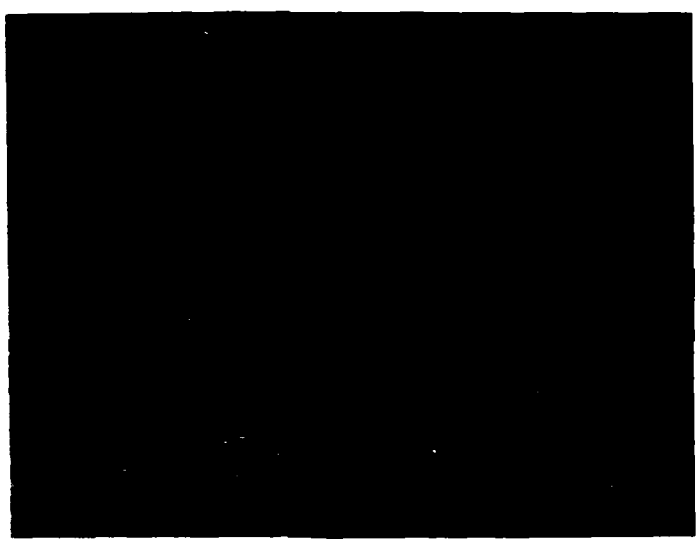

Figure 15. A typical interface (560X)

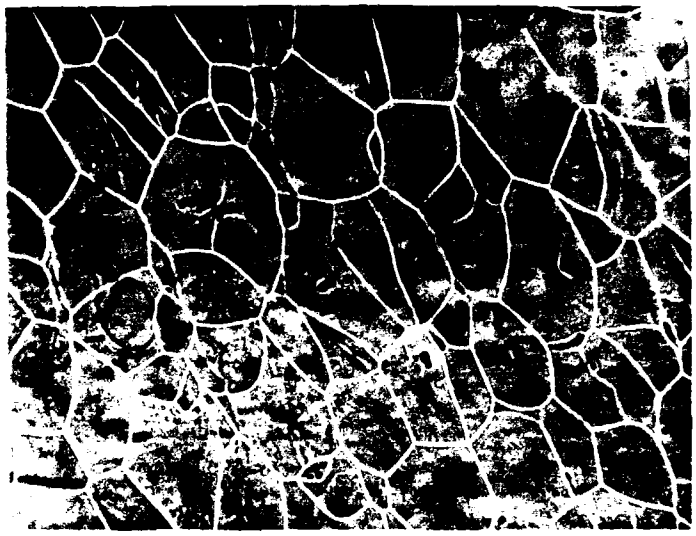

Figure 16. A typical surface of epitaxial InP (110X)

and decent growth rates. The electrical properties of these layers are discussed in the next section.

5.3 RESULTS OF ELECTRICAL EVALUATION

5.3.1 Schottky-Barriers

Initial efforts to evaporate Al onto clean InP resulted in Schottky diodes that had very high leakage currents. Many were almost ohmic, and most were found to be unsuitable for doping profile measurements. In an attempt to lower the leakage by lowering the measurement temperature a simple probe station which could be submerged in liquid nitrogen was constructed and tested. Due to unstable contacts on the probe, the leakage current decreased only slightly. This effort was abandoned and the use of an oxide layer examined.

A second set of samples was etched just prior to evaporation. The etch consisted of submerging the sample in steaming "aurostrip" for five minutes followed by a rinse with methonal. The resulting barriers were significantly better than previous ones. The leakage current was reduced and C-V readings were stable.

The I-V characteristics for a gold MIS structure are given in Figure 17. The current remains below 5 μA at a reverse bias of 4 volts. Most of the gold Schottkies evaporated onto the same substrate were of sufficient quality to be used for C-V measurements. The process of etching in aurostrip before evaporating gold contacts resulted in the best rectifying contacts obtained.

Al MIS barriers were also fabricated by etching with aurostrip. Representative I-V curves are shown in Figure 18. Here the reverse current is less than 20 μA out to a reverse bias of 5 volts. The

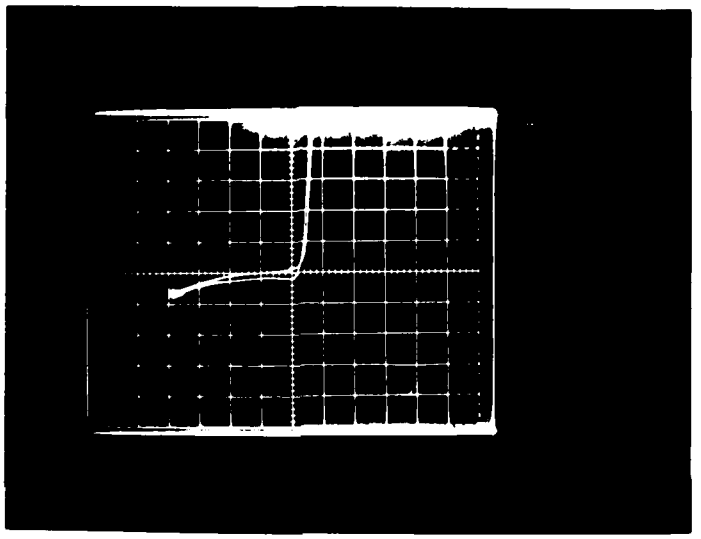

Figure 17. I-V characteristics for Gold/InP MIS Schottky diode.

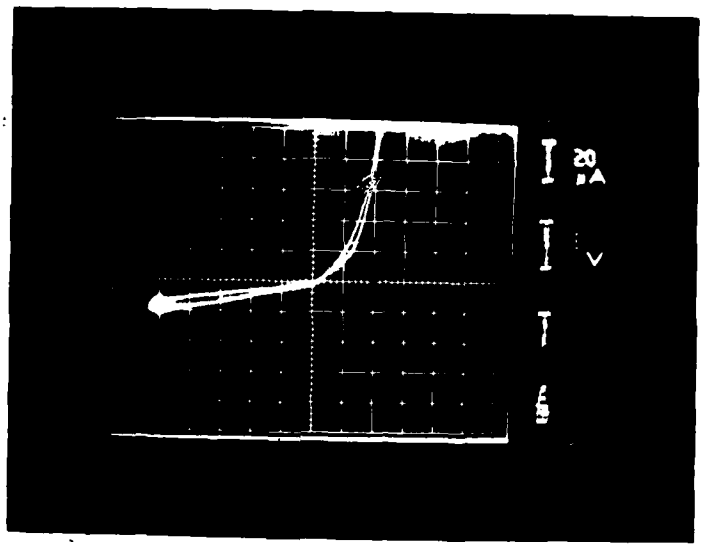

(a)

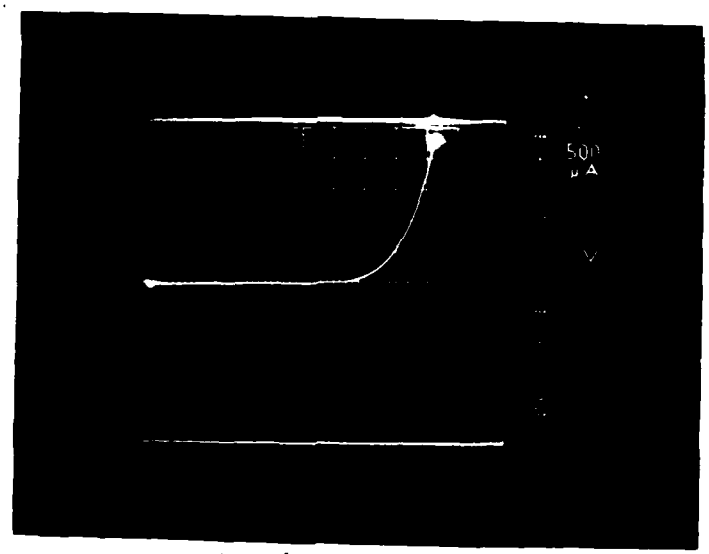

(b)

Figure 18. I-V characteristics for Al/InP MIS Schottky diode

effective barrier height for Al is less than that for Au but is sufficient for accurate C-V measurements or for use in other devices.

Techniques for creation of an oxide layer by sintering in air were also investigated. The results are shown in Figure 19 and 20. Figures 19a and 20a show the I-V characteristics of a Schottky diode fabricated by evaporating Al onto an InP surface that had been exposed to the atmosphere but not etched (i.e. there was no intentional layer of oxide present at the interface). The barrier height was low and the diode close to ohmic. After heating the device at 250°C in the air for 30 minutes the I-V characteristics were as shown in Figure 19(b) and 20(b). The reverse characteristics now go out to -1.2 volts before breaking down. The forward current is affected by the series resistance of the oxide at higher currents. Both of these effects indicate the presence of an interfacial oxide layer. Thus sintering in air presents another technique for increasing the effective barrier height of an Al/InP contacts.

Comparison of Figures 18a and 20b leads to an understanding of the thickness of the oxide layer which presents a series resistance that will increase as the thickness of the layer increases. This series resistance is important at high current levels because the voltage drop across the oxide becomes significant. If the voltage drop across the oxide is no longer negligible compared to the drop across the depleted region then the terminal voltage cannot be assumed to be equal to the voltage of the depleted region. The reduced voltage across the depleted region reduces the reverse saturation current.

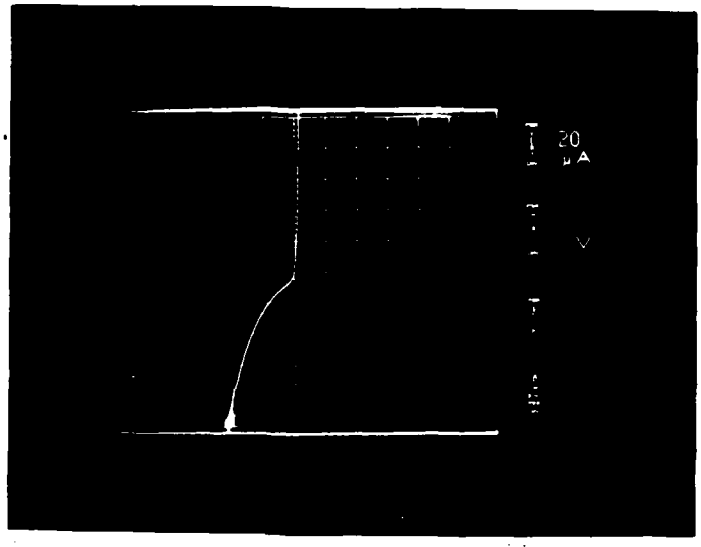

a) I-V characteristics of Al/InP barrier before annealing

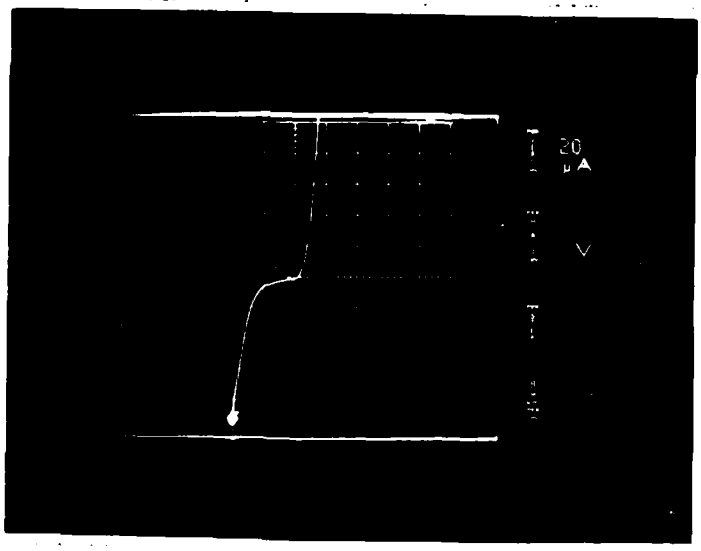

b) I-V characteristics of same Al/InP barrier after annealing in air at 250°C for 30 minutes

Figure 19. Effect of Annealing on reverse saturation current of Al/InP barriers

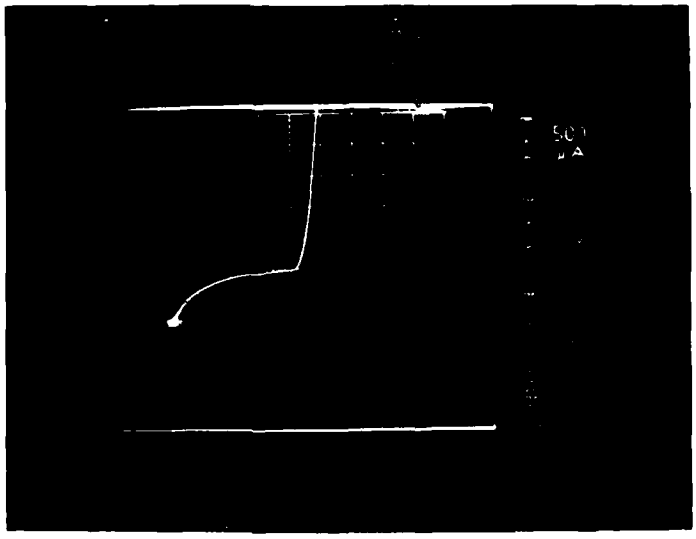

a) I-V characteristics before annealing

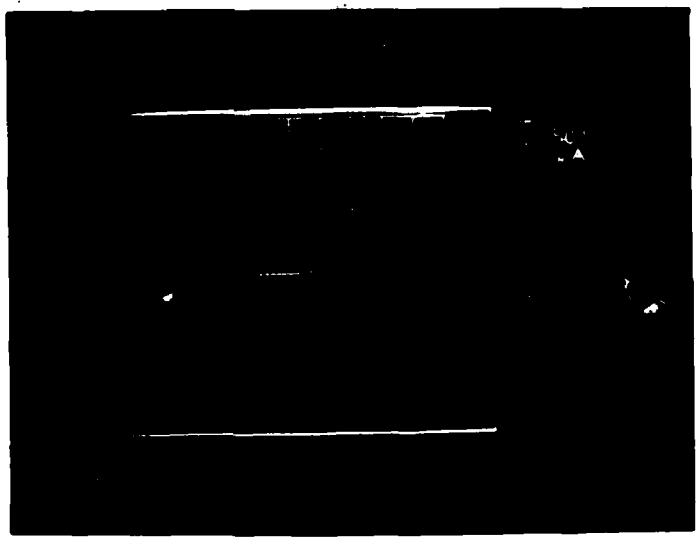

b) I-V characteristics after annealing diode at 250°C for 30 minutes in air

Figure 20 Effect of Annealing Al/InP barriers (forward characteristics)

The oxide layer flattens out the forward characteristic and effectively shifts the forward curve to higher voltages. In Figure 28a, the diode reaches a current of 2mA at 0.8 volts. This is with no oxide layer. After forming an interfacial layer of oxide by annealling, the diode's forward characteristics are as shown in Figure 20b. Because of the resistance of the oxide layer, the diode does not reach a current of 2mA until the voltage is 2.4 volts. The diode in Figure 18 does not reach a current of 1mA until the terminal voltage is 4 volts. The oxide layer created by etching in aurostrip apparently is thicker or has a higher resistivity than the one formed by sintering.

5.3.2 Doping Profiles

Doping profiles were obtained using aluminum MIS contacts. Figure 21 presents the doping profile of Sample 9, which was undoped. Most of the layer was depleted at zero bias, implying lightly doped material. The I-V curve was also sensitive to light, again implying light doping. The C-V measurements revealed an increase in carrier concentration from $6x10^{13}$ cm^{-3} at a depth of 3.7μm to $1.1x10^{16}cm^{-3}$ at 4.1μm from the surface. At higher voltages, the C-V measurements failed because of the high concentration in the substrate and breakdown of the diode at that bias.

Sample 10 (unintentionally doped) was compensated; the I-V curve was characteristic of a npn structure. Hall measurements made on a sample simultaneously grown on a semi-insulating substrate also revealed compensated material with a low mobility. Poor contacts to the Hall measurements prevented accurate measurements of the exact

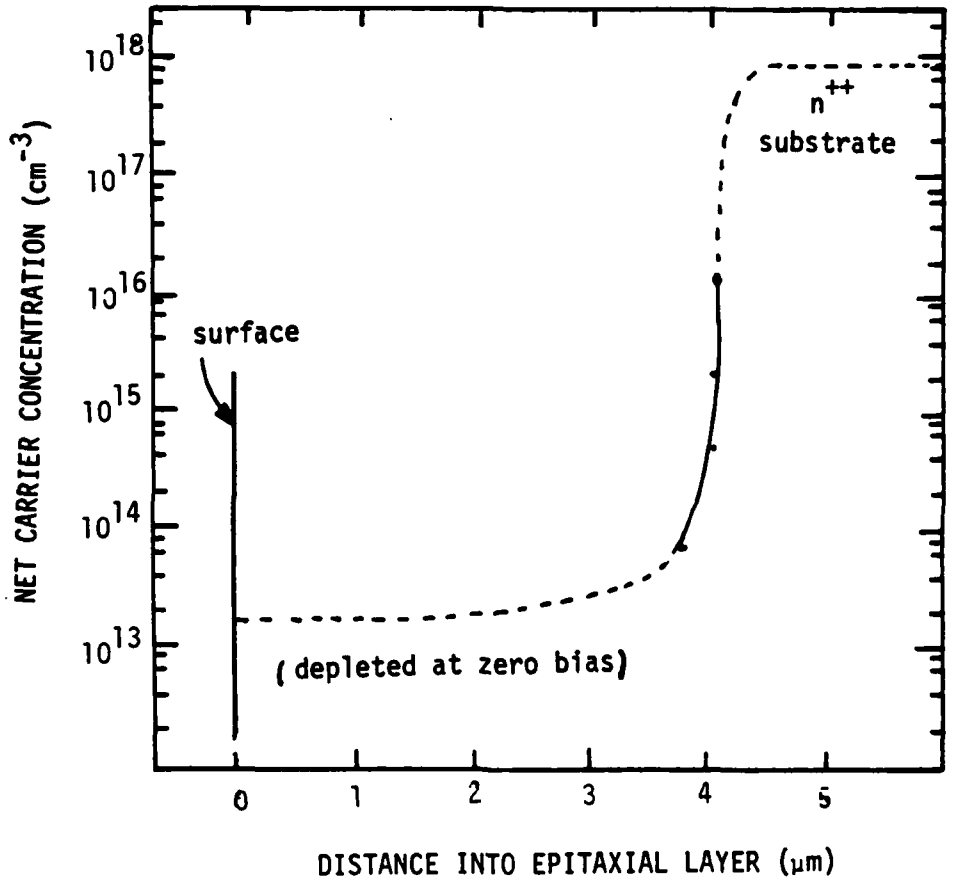

Figure 21: Doping profile for undoped InP epitaxial layer

mobility or concentration. Attempts to make new contacts were unsuccessful due to the small substrate size.

Sample 11 was intentionally doped with H_2S. Its doping profile, obtained by step-etch techniques, is given in Figure 22. The H_2S dopant was introduced upstream from the substrate at a flow of 0.1 ml/min for the first few μm of the epitaxial layer. A layer of undoped material was grown on top of that. An H_2S flow rate of 0.1 ml/min produced a donor concentration of $1.0 \times 10^{15} cm^{-3}$ that was uniform throughout the doped portion of the layer.

Tests are currently being performed to determine the dependence of donor concentration on H_2S flow rates. Both Clarke [26] and Chevrier [2] found a linear relationship with a slope of unity. The only difference between their results was a shift in the curve corresponding to the background doping level of each reactor. Assuming that this relation will hold for this system a curve of doping vs H_2S flow is postulated in Figure 23. Work is in progress to verify this relationship.

Judging by the uniform doping level obtained in Sample 11 and by the findings of other workers, controlled doping with H_2S should be relatively straightforward. The double dilution dopant system allows accurate control of the low level of H_2S dopant flows necessary to achieve light doping (i.e. 0.01 ml/min). This accurate control of H_2S flow will yield corresponding control of doping concentration in the grown layers.

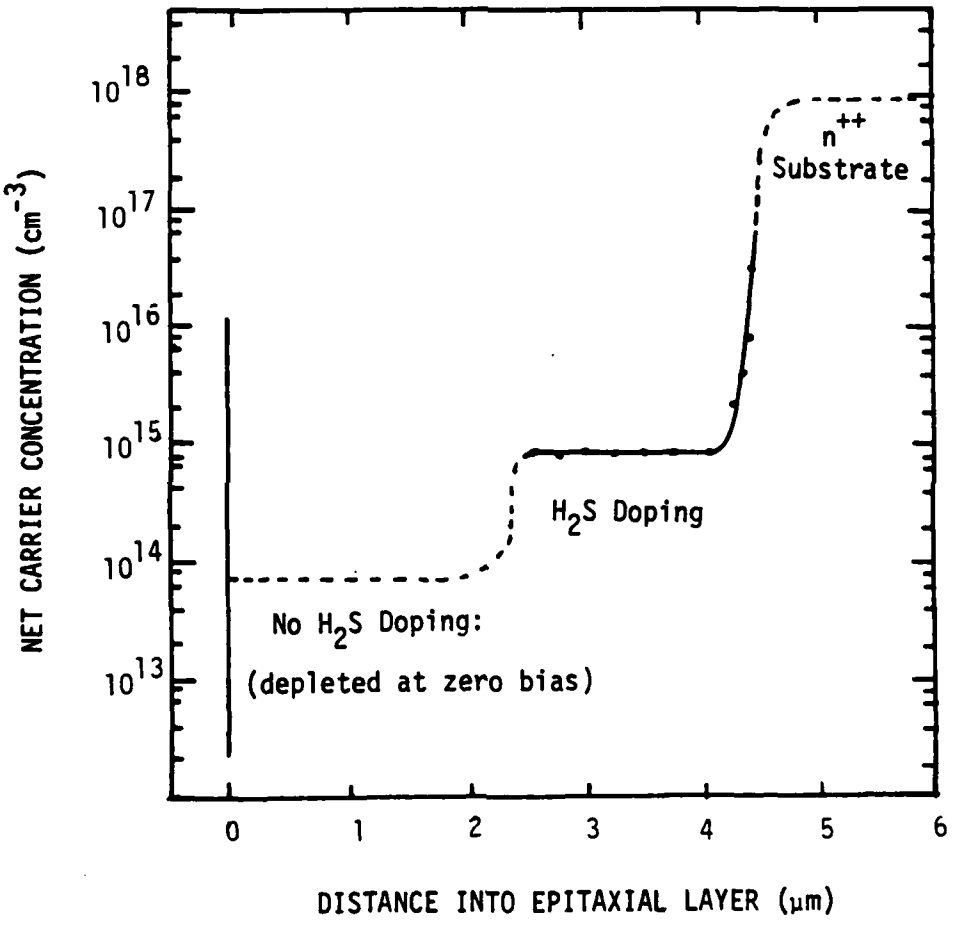

Figure 22: Doping profile of H_2S doped InP epitaxial layer determined by C-V measurements.

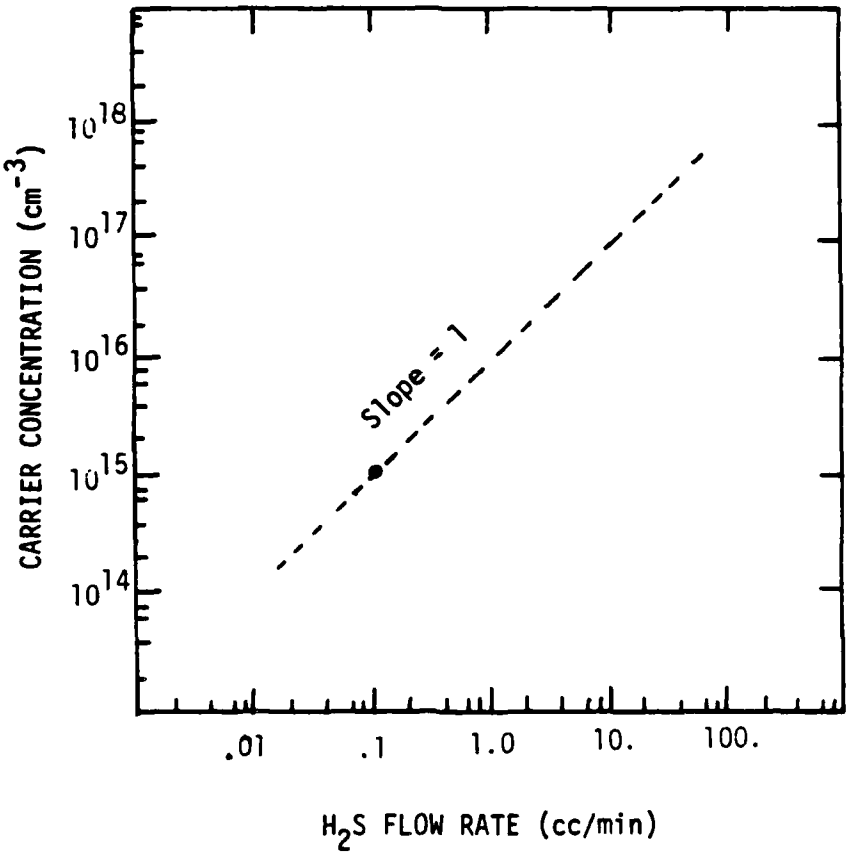

Figure 23: Postulated H_2S flow rate versus Carrier Concentration

6. CONCLUSIONS AND RECOMMENDATIONS

Problems associated with the VPE growth and evaluation of device grade InP have been investigated. A complex reactor system capable of double dilution doping to achieve accurate H_2S doping even at low levels has been designed, assembled, and used to grow several samples. Major factors affecting the epitaxial growth process were investigated, including PCl_3 mole fraction, temperature profile, and flow rates. Standard growth conditions were established.

The grown material was evaluated for its physical and electrical properties. Layers with smooth surfaces, good interfaces and uniform thickness were obtained. The growth rate, primarily governed by the rapid depletion of the melt, was found to be approximately 20 μm/hr. Material with residual doping concentrations of $1x10^{14}cm^{-3}$ was obtained. Controlled H_2S doping resulted in predictable and uniform carrier concentration with depth.

The problem of Schottky diodes on InP was addressed and a satisfactory answer found. The barriers may be improved by inserting a thin oxide layer between the semiconductor and metal. The resulting MIS structure behaves as a normal Schottky diodes with higher effective barrier height if the oxide layer is thin. This layer may be fabricated either by etching prior to the metal deposition or by sintering the diode after metalization. Research is needed to gain better control over the oxide thickness and hence the barrier height.

In general no major obstacles are present which prevent InP from being grown in device grade quality. Such actions as purging with Ar before the tube is open, removing large quantities of waste from the

tube after each run and the need for an MIS structure to measure doping profile are all inconvenient but certainly not prohibitive. Although research into InP growth parameters and device fabrication is still necessary to refine the technology, the high potential for InP is certain, especially in millimeter wave applications.

The equipment and techniques reported here can be utilized in continuing efforts to grown controlled epitaxial material for use in devices. One particular aim is fabrication of a sample for v(E) measurements, which requires an aluminum Schottky diode.

6.2 SAMPLE FOR v(E) MEASUREMENTS

A cross sectional view of such a v(E) sample is shown in Figure 24. An InP epitaxial layer is grown on a highly doped InP substrate by the PCl_3-In-H system. The diode consists of a thin aluminum window and a thick aluminum annulus. In the electron-beam velocity field apparatus, described elsewhere [25], electrons are injected through the thin window when their energies are above a critical value that is determined by the contact thickness. The thick annulus provides a good mechanical region that permits ultrasonic wire bonding to the Schottky contact. The substrate contact is made using an alloyed gold-germanium nickel layer. A thick layer of plated gold is added to permit thermal compression die bonding of the sample to a gold plated copper stud.

Such a diode needs accurate control of doping to achieve a profile such as in Figure 25. It also needs a low leakage Schottky contact of InP and aluminum, which will require some form of interfacial oxide layer. Calculations to assure that the oxide layer

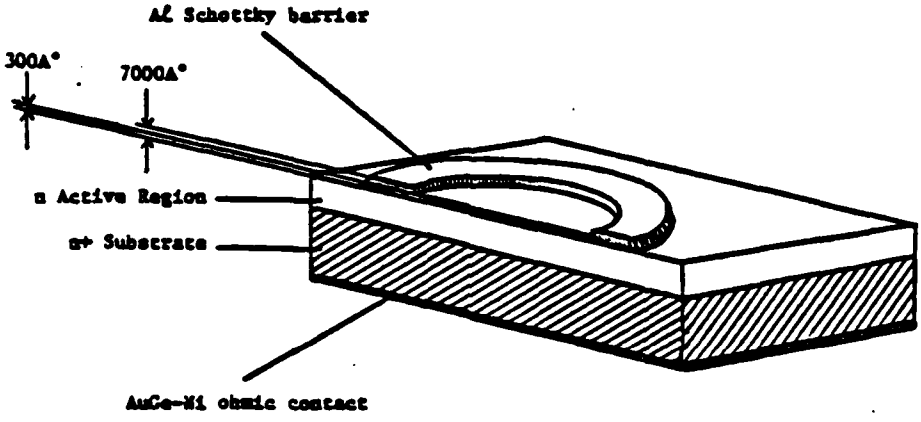

Figure 24. Cross sectional view of sample for velocity-field measurements

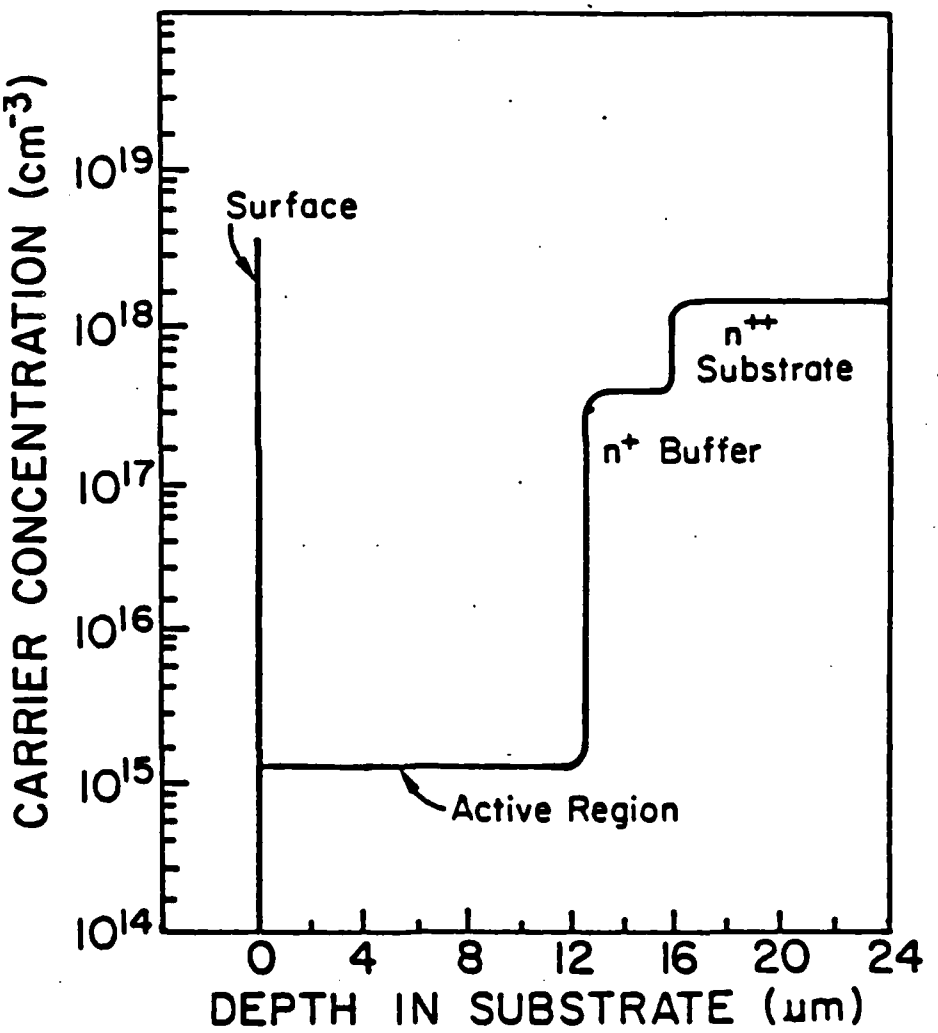

Figure 25. Doping profile for velocity-field measurement sample.

necessary for a decent barrier does not affect the velocity field measurements may be necessary.

6.3 RECOMMENDATIONS FOR FUTURE WORK

Although many problems concerning the growth and evaluation of device grade InP have been solved, others still require attention. The following is a summary of some useful improvements in techniques or equipment.

6.3.1 Growth Techniques

(a) Reduce the temperature variation across the source. As discussed earlier a temperature gradient across the source increases the impurity concentration of the grown layer in a manner which is difficult to control. A decrease in the temperature variation over the source will increase the reproducibility of results obtained. Presently the temperature varies $\pm$ 0.5°C, compared to the desired goal of $\pm$ 0.1°C.

(b) Grow Hall effect samples on semiinsulating substrates along with n^{++} substrates. The Hall measurements will give a check on donor concentration and provide mobility data. This extra data is useful in fine tuning the reactor to produce pure, high mobility, uncompensated material. The donor concentration given by Hall measurements may also be compared to C-V measurements done on n^{++} substrates to check the accuracy of the latter technique.

(c) Reduce the amount of oxygen in the system by sealing any new leaks and/or replacing the PCl_3 liquid in the bubbler which

may be contaminated by P_2O_3. Further reduction of O_2 may be accomplished by covering the entire control board assembly with a plexiglass container and flushing it with N_2 gas. This precaution would reduce the amount of O_2 leaking into the system at tubing connections and joints by aspiration.

6.3.2 Schottky Barriers

(a) Use gold MIS structures for C-V measurements, but experiment with aluminum contacts for use on other devices.

(b) Find a better etch for doing step-etch C-V analysis of thick epitaxial layers. The use of 1% bromine methonal provides rough surfaces. The literature suggests the use of 5:1:1 H_2O_2-H_2SO_4-H_2O before etching in bromine methonal to obtain better surfaces. A study is also needed of etch rate of bromine methonal solutions on InP [28,29] in order to accurately control the depth of the etch into the epitaxial layer.

(c) Try the mercury probe for C-V measurements. To use this device, the back side of the sample must be lapped down with 5μm grit. This is done to insure that no InP from the top epitaxial layer curves around the side and shorts out to the bottom side. The sample should then be etched smooth so that the probe can make a good ohmic contact on the back and a good Schottky barrier on the front side. The etch should also deposit an oxide layer on the top surface to assist in forming an interfacial layer for the barrier. A bromine-methonal etch is suggested.

(d) Refine the 77°K C-V measurements by refining the cold temperature probe station. The present jig is inadequate.

(e) The oxide layers in the MIS Schottky barriers seem to breakdown at reverse voltages with magnitudes greater than five or six volts. This effect may be studied further in the hope of creating barriers that are good at higher reverse voltages.

ACKNOWLEDGEMENT

The authors appreciate the expertise in crystal growth supplied by Jerome Teng, Roger Green, and Gary Davis. Also, special thanks are due to Mack Morman who assisted in assembling various subsystems used in the main reactor. Thanks also to Mr. Gus Weinstock for his support.

8. APPENDICES

APPENDIX 8.1

STEP BY STEP PROCEDURES

8.1.1 Procedures for VPE Growth of InP

1. Turn on furnace via circuit breakers "A" and "B" in fuse box. Takes approximately 1.5 hours to stabilize to set points.
2. Turn on argon purifier ["hydrox"]. A few minutes later switch ARGON/HYDROGEN valve to ARGON. Set very high flows to flush system, especially reaction tube, with argon to expel any hydrogen. Tube must be flushed with argon at greater than 200 ml/min for 15 minutes before opening tube.
3. Prepare substrate:
   - A. Cleave sample size substrate (approximately one square centimeter) from InP substrate stock.
   - B. Clean with organics in following order:
     - a) TCE
     - b) Acetone
     - c) Methynol
   - C. Etch for 4 minutes in 2% Bromine-methanol solution. [Recommend 49 ml methanol/1 ml bromine]
   - D. Flush thoroughly with methanol.
   - E. Leave in methanol until just prior to insertion into furnace.

4. Place substrate into reaction tube:

   A. After argon flush is complete (15 minutes or more), turn up argon flow to maximum flow rate and open end of reaction tube (take off end cap).

   B. Take sample out of methanol, dry on bibulous paper, and place on sample holder.

   C. Insert sample holder into reaction tube and push to desired position in tube.

   D. Replace end cap. Let argon flow continue for about 5 minutes at a moderate flow rate until switching system back to hydrogen.

5. Purge system with hydrogen. Reaction tube must have flow of at least 200 ml/min for at least thirty minutes.

(After furnace temperatures have stabilized and reactor has purged with hydrogen sufficiently then continue).

6. Roll furnace over reaction tube to correct position. (Remember to open furnace doors on reactor side first!) Record time.

7. Set flows in order to resaturate the melt. Turn on PCl_3 bubbler. Allow approximately ten or twelve minutes for resaturation to occur. During this time the furnace temperatures should restabilize. Record time bubbler turned on and all significant flow rates.

8. Grow epitaxial layer. Adjust flow rates as required. Growth time depends on layer thickness and growth rate.

9. Turn off PCl_3 bubbler and roll furnace off of tube to terminate epitaxial growth.

10. Wait about five minutes for reaction tube to cool, then begin flushing with argon. Purge tube for at least fifteen minutes before opening.

11. Open reaction tube. Scrape deposits off reactor wall that built up during growth run.

12. Once tube is sufficiently clean, pull sample holder out of tube. Place sample in covered petri dish.

13. (Optional) Place new sample substrate on sample holder and position again in reaction tube.

14. Replace end cap. Wait five minutes. Reestablish hydrogen flows. (Low flow rate for dormant system or high flow rate if next growth run is done immediately).

[Shutdown to "dormant" status]:

15. Turn off furnace. Set hydrogen to very low flow rates.

8.1.2 Procedure for C-V Analysis Using Evaporated Schottky-Barriers

A) Pre-evaporation etch:

1) Fix sample, with epitaxial layer up, on a glass slide with black wax.

2) Clean with TCE, acetone, and methanol.

3) Heat up beaker of aurostrip until steaming.

4) Place sample in steaming aurostrip for five minutes.

5) Rinse with methanol.

B) Evaporation

1) Load gold or aluminum into RDI evaporator.

2) Place mask over sample(s) so that half of the sample will have a solid coating of metal with the other half as ~~bits~~.

3) Pump down chamber to less than 7×10^{-6} torr before deposition.

4) Deposit about 2000A of metal onto surface.

5) Remove sample from RDI.

C) Analysis:

1) Connect probe station to curve tracer and C-V profiler.

2) Place one probe on large pad, another on any individual dot (Schottky).

3) Check I-V curve for low leakage diode. If diode is not too leaky, then proceed with profiling measurements.

4) Check polarity of bias on diode: Check the zero-bias capacitance. Increase the reverse bias voltage and monitor the capacitance. If the capacitance decreases then the diode is properly biased. If it begins to increase, switch the polarity.

5) Take the C-V data manually and use Equations (10) and (11) to obtain the doping profile or else use the automatic doping profiles.

D) Step-Etch Technique

(If the profile does not punch through the epitaxial layer).

1) Strip off present metalization with HF or aurostrip.

2) Clean with organics.

3) Cover part of sample with black wax to protect it from the etch.

4) Etch in 1% bromine-methanol solution. Etches about 5μm per minute.

5) Remove the cover wax with organic solvents.

6) Measure the amount etched by using a high power optical microscope, focusing on each side of the step, and comparing the vertical distance between the two focus positions on the microscope.

7) Put new Schottky diode on the etched surface (repeat steps A, B, and C).

8.1.3 Operating Procedure for RDI Evaporator System

A) 1) With roughing valve closed, bleed bell jar. This entails opening valve on rear N_2 cylinder, opening paddle valve marked 'RDI', and opening bleed valve on RDI until gas flow is audible. When bell jar is bled, it will pop up off the base slightly. Close bleed valve.

2) Raise bell jar slowly. When it hits the vent, push it over and continue raising.

3) Remove sample holder, chimney (if on), lid and base to evaporator cover.

4) Remove old basket and discard. Replace with new basket making sure there is no torque it.

5) Fill basket with Al. A 6 inch length cut into 1/2 inch pieces is used. The bottom end of the first piece put in the basket should be doubled over to plug the hole in the bottom of the basket.

6) Mount samples in the sample holder.

7) Reassemble cover making sure not to short the electrode with the cover or the Al foil. Replace sample holder and chimney if desired.

8) Slowly lower bell jar.

9) Rough bell jar.

B) Pump Down Procedure

1) Rough oil diffusion pump (foreline).

2) Turn on oil diffusion pump.

AD-A120 551 VPE GROWTH OF INP FOR ELECTRONIC DEVICES(U) WASHINGTON 2/2
UNIV ST LOUIS MO DEPT OF ELECTRICAL ENGINEERING
J M BORNHOLDT ET AL. MAY 82 82-2-ONR N00014-79-C-0840
UNCLASSIFIED F/G 9/5 NL

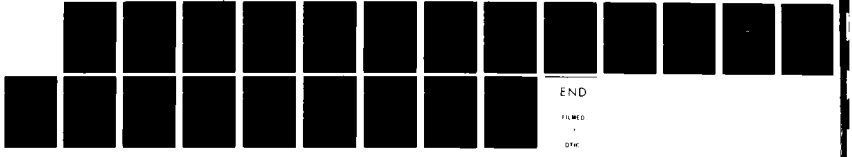

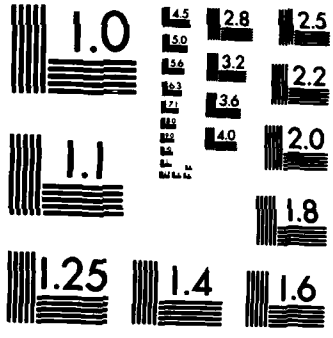

MICROCOPY RESOLUTION TEST CHART
NATIONAL BUREAU OF STANDARDS-1963-A

3) Close foreline valve.

4) Rough sample chamber (open roughing valve).

5) Close roughing valve.

Open foreline valve.

Open high vacuum valve.

6) Degas ionization gauge - 5 minutes.

7) After degassing, turn on ionization gauge.

8) Fill cold trap with LN_2.

9) Let pump down 3-4 hours.

C) Deposition

Make sure shutter is closed (handle towards user)

1) Refill cold trap with LN_2. Turn off ionization gauge.

2) Turn on evaporator power supply.

3) Turn up power until current is around 30A (may take a couple of minutes until filament glows).

4) Watch basket for aluminum melting and falling to bottom (turn off lights).

5) After this happens turn current up to 50A.

6) Open shutter.

7) Deposit to desired thickness or until aluminum is gone.

8) Close shutter.

9) Turn off evaporator power. Close high vacuum valve.

10) Bleed chamber.

11) Remove samples.

12) Rough chamber (foreline valve closed!)

13) Close roughing valve, open foreline valve.

14) Turn off diffusion pump.

15) About an hour later turn off mechanical pump (after shutting foreline valve).

D) Thickness Moniter: (Use during deposition)

1) Turn on both thickness monitor and tine monitors.

2) Set material variable to correct setting (Al:N=320, Au:N=50)

3) "Zero" moniter.

4) Press "test"; record value.

5) Before opening shutter, press "start"; will record time and thickness.

6) Press "stop" when finished with deposition.

7) Record "test" value. Should be seen of previous value plus layer thickness.

APPENDIX 8.2

Use of the Double Dilution Dopant System

The double dilution dopant system allows accurate control of the H_2S dopant flow below 0.01 ml/min. A schematic is given in Figure 8.2.1. The H_2S out of the tank is controlled by an electronic mass flow controller which will regulate the flow, f_A, from one to fifty ml/min. This flow is mixed with flow f_B which is hydrogen controlled by an another mass flow controller. Flow f_B can be regulated between 10 and 500 ml/min. The mixture of flows f_A and f_B is denoted by f_{AB}. Part of this mixture is vented out to the exhaust through a needle valve. The resulting flow through the rotameter, f_D, can be adjusted so that flow f_D is some fraction of flow f_{AB}. Therefore:

$$f_D = K_1 f_{AB} = K_1(f_A + f_B) \equiv \text{"MIX I" (primary dilution)} \tag{1}$$

where $f_A \equiv$ flow of H_2S $\quad (1 \leq f_A < 50)$ ml/min

$f_B \equiv$ flow of H_2 $\quad (10 \leq f_B \leq 500)$ ml/min

$K_1 =$ arbitrary constant $(0 < K_1 < 1)$

This primary dilution mixture, f_D, is again diluted with another hydrogen flow, f_E, to form the combined flow, f_{DE}. Part of this flow is vented to exhaust so that the final flow, f_G, can be regulated by the rotometer. Flow f_G is a fractional part of F_{DE}, so:

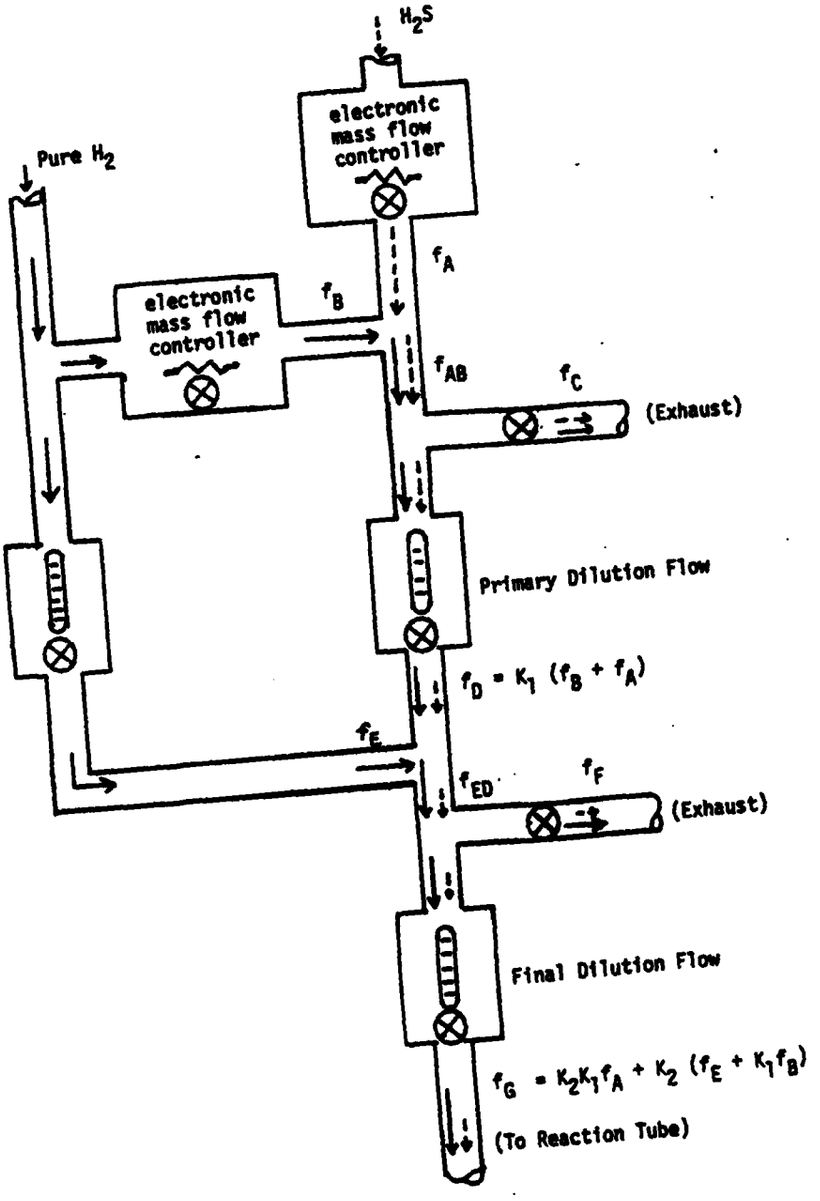

Figure 8.2.1: Schematic of Double Dilution Flow System

$$f_G = K_2 f_{DE} = K_2(f_D + f_E) \equiv \text{"MIX II"} \qquad (2)$$

where $0 < K_2 < 1$

Combining Equations (1) and (2) yield:

$$\underset{\text{dilution}}{\text{final}} = f_G = K_2 * K_1 * f_A + K_2 * (K_1 f_B + f_E) \qquad (3)$$

H_2S flow $\qquad$ H_2 flow

Equation (3) can be used to determine the required flows and dilutions necessary to achieve a desired final flow of H_2S in any given final total flow through the dopant line, f_G.

Example: A H_2S flow of 0.5 ml/min in a total flow of 20 ml/min in the dopant line is desired.

Choose: $K_1 = K_2 = 0.1$ (arbitrary)

From Equation (3): $f_A = \frac{fH_2S}{K_2 + K_1} = \frac{.05}{(.1)(.1)} = 5$ ml/min

Since $0.05 \leq 20$, f_C is primarily hydrogen, so Equation (3) becomes:

$$f_G \approxeq K_2(K_1 f_B + f_E)$$

$$.1\, f_B + f_E \equiv 200 \text{ ml/min}$$

Choose f_B = 200 ml/min, then $f_E \cong 200-20 \equiv 180$ ml/min

From (1), $f_D = K_1(f_A + f_B) = (.1)(205) = 20.5$ ml/min

Actually, any values of K_1, K_2, f_E, f_D, and f_B may be used as long as none of the other parameters exceed their physical bounds set by the capacity and precision of the flow controllers and rotometers.

APPENDIX 8.3

Chemical and Temperature Effects During Saturation

8.3.1 Chemical Effects

Besides reaction (2) ($4In+P_4 \rightarrow InP$) there are other reactions that occur during source saturation [4,5,22]. Besides reacting with the P vapor to form InP the In in the source also reacts with the HCl gas from the dissociated PCl_3 (reaction 1) to form InCl. This may be expressed by the following reaction:

$$2HCl + 2In \xrightarrow{750°C} 2InCl + H_2 \qquad (16)$$

This reaction is significant in the saturation process because it depletes indium from the unsaturated melt. The InCl is transported down the reaction tube and condenses as a black or orange solid. Large amounts of this material condenses on the sides of the tube after a saturation and must be scraped off before a seed can be entered. During saturation most of the P vapor is absorbed into the melt and most of the Cl is converted into InCl. For every mole of PCl_3 dissociated there results one mole of InP and three moles of InCl. Since the solubility of InP in indium (Figure 5) is 0.07 at 700°C then approximately 21 percent of the indium source will be lost during saturation.

Once the source is completely saturated and is covered by a skin of InP other reactions occur. At temperatures in excess of 380°C the vapor pressure of phosphorous over the solid InP rises rapidly causing

phosphorous loss and an indium rich surface. This reaction may be written as:

$$4InP \xrightarrow{750°C} 4In + P_4 \qquad (17)$$

Reaction (17) is the reverse of reaction (2).

Reaction (17) can be combined with reaction (16) to give the transport reaction:

$$4HCl + 4InP \xrightarrow{750°C} 4InCl + 2H_2 + P_4 \qquad (4a)$$

Note that combining Equations 16 and 17 results in cancellation of elemental indium from both sides of the reaction. The In created by reaction (17) is simultaneously converted into InCl by reaction (16). The net result is that the HCl gas reacts with InP to form phosphorous, indium chloride and hydrogen. These products are transported down the tube to a cooler region around 650°C where the reverse of reaction (4a) occurs and InP is deposited on the seed or the walls of the reaction tube. Polycrystalline InP on the reactor walls appears as a light grey material.

If there are no temperature variations across the source, a thin skin of InP will continue to cover the source throughout its useful life. The InP removed by the HCl via reaction (4a) will be replaced by absorption of P_4 into the source to form InP via reaction (2) and saturation is maintained. The thickness of the crust depends on the partial pressure of the phosphorous vapor over the saturated source [5].

The source must be resaturated every growth run. This occurs partially because the cooled melt has formed a crust of precipitated InP which must dissolve back into the source when it is heated to growth temperatures [4]. While this is occurring the indium melt is absorbing phosphorous vapor from the gas flow. This pre-saturation condition occurs for about ten minutes until the melt is fully saturated. Only after the source is saturated will the growth reactions occur. Thus there is a ten minute lag between the time that the PCl_3 flow over the melt is established and the time that growth actually begins.

Since the substrate is elevated to high temperatures during the resaturation period, phosphorous can leave the indium phosphide seed surface by reaction (17). This leaves a pitted, indium rich surface that is unsuitable to grow a layer on. The problem is relieved by the presence of HCl over the seed which etches the damaged surface (reaction 3a) until the source is resaturated and growth begins. The excess HCl is present in the gas flow past the source because a large part of the phosphorous vapor is absorbed into the source. After saturation the HCl over the source becomes involved in reactions (4a) and (4b) so little etching at the seed occurs.

8.3.2 Effect of Temperature Gradient

If there are temperature variations along the source the In/InP solution can only be saturated with respect to the lowest temperature. Thus convection and solid migration will occur. The phosphorous will be absorbed from the vapor at warm point and indium phosphide will precipitate at cool point. The absorption of phosphorous during

recede off the warm points exposing the indium [5]. These areas will appear shiny. Areas that are cooler will have a gray InP crust over them. As the source cools and InP is precipitated out from all areas of the source the warmer areas will precipitate out more InP than the cooler areas. Thus the areas that are shiny at elevated temperatures may appear gray at room temperature and those areas that are gray at elevated temperatures may appear shiny at room temperature. Therefore it is important to observe the source while it is still hot.

Several observations of the hot source immediately after growth or saturation were made. In Figure 8.3.1 the surface of the melt is compared to the growth temperature profile across the source. The portions of the source at slightly higher temperatures appeared smooth and shiny. The InP crust had receded from these points exposing the indium. The lower temperature regions of the melt were dark gray, indicating the existence of an InP crust in these areas. The edge of the boat lying on a step downward temperature gradient contained only precipated InP. The source depleted rapidly in the high temperature gradient areas. This is caused by the loss of indium converted to InCl (reaction 16) in this unsaturated region. All these effects are caused by temperature gradients across the source.

If there are not temperature gradients the source should have a uniform skin of InP covering the melt. Thus observations of the hot source with and without the PCl_3 flow can aid in determining the existence or extent of temperature variation across it.

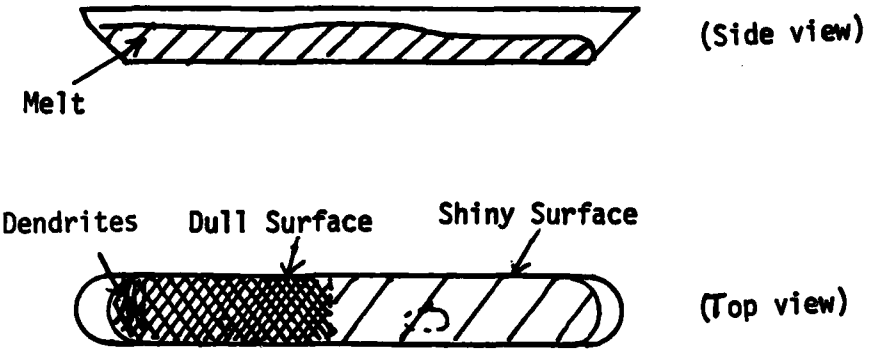

(a) Indium Source Boat after Growth Run

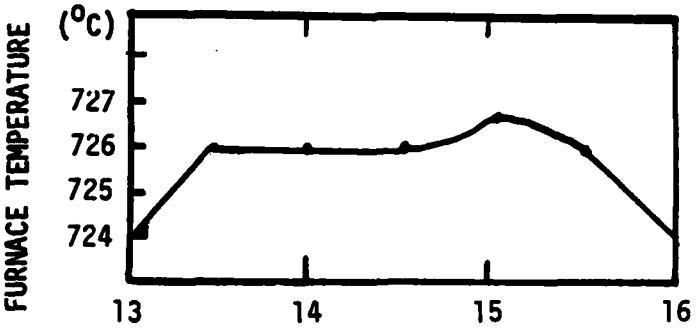

(b) Furnace Temperature Profile

Figure 8.3.1 Effect of temperature variations on source melt

APPENDIX 8.4

SUBSYSTEM SCHEMATICS

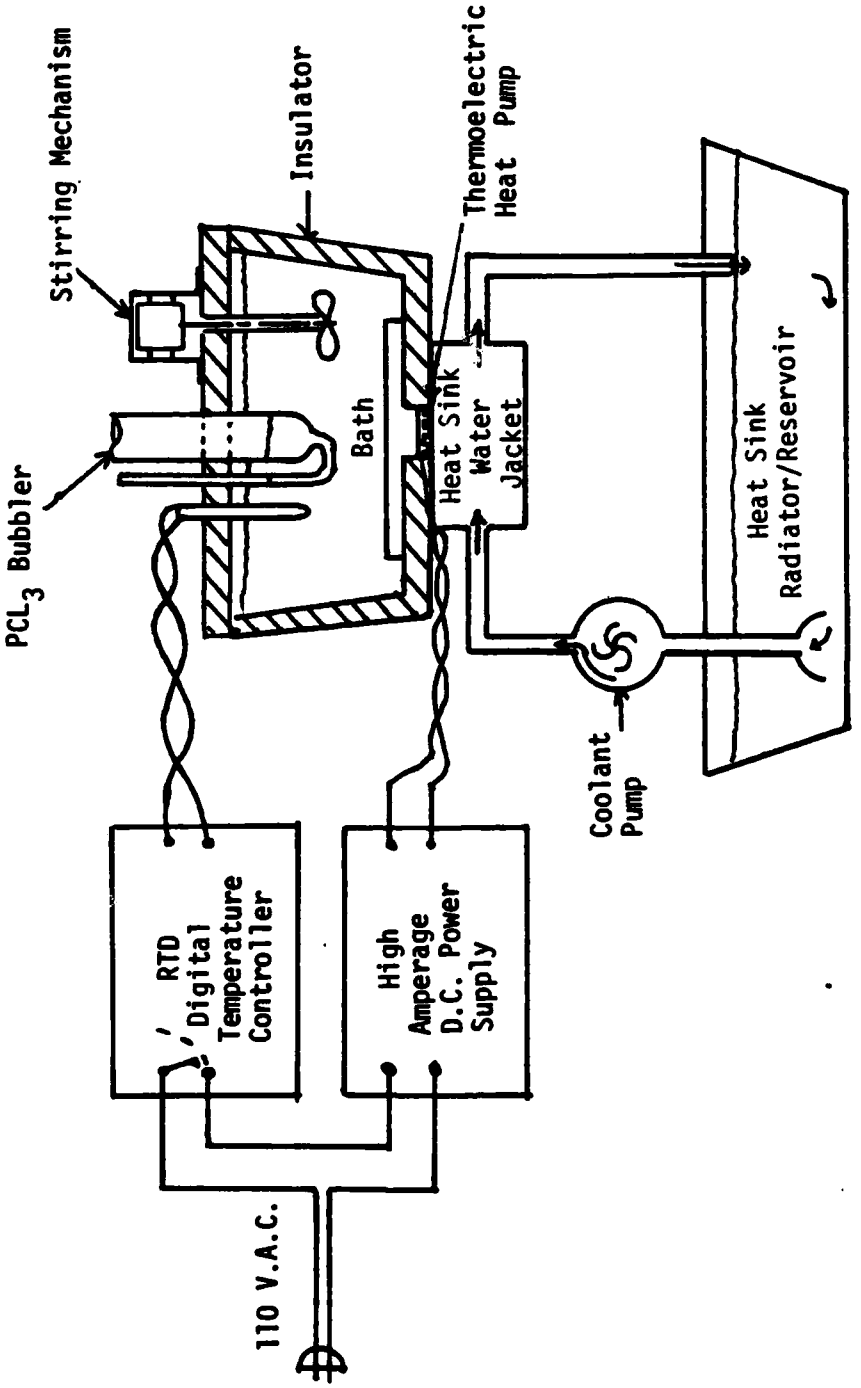

Figure 8.4.1 Schematic of Thermoelectric Cooler System

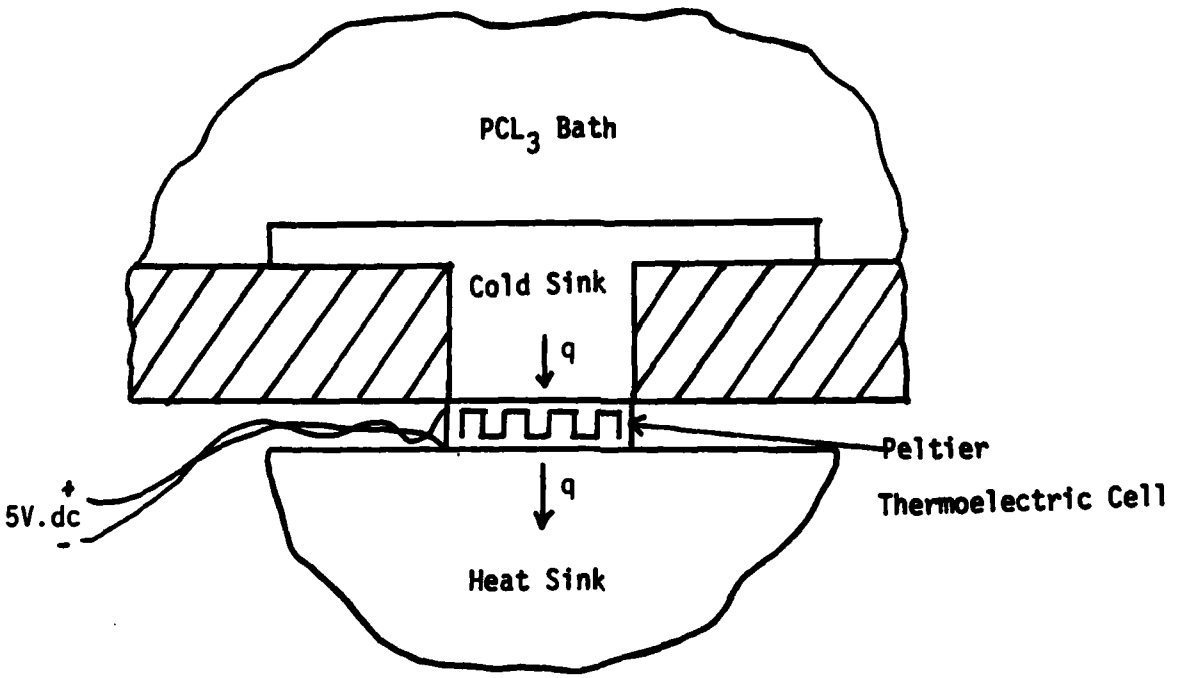

Figure 8.4.2. Detail of Peltier Cell as a heat pump in the thermoelectric cooler

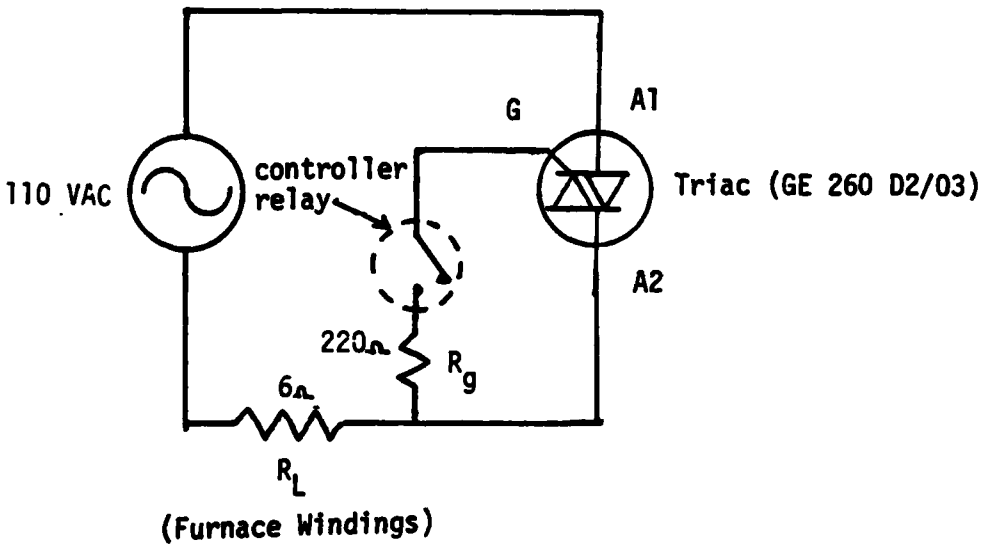

Figure 8.4.3 Triac circuit used to control furnace

9. BIBLIOGRAPHY

1. R.D. Fiarman, M. Omori and F.B. Frank, "Recent progress in the control of high purity VPE InP by the PCl_3/Ind H_2 technique" Institute of Physics Conference, Series No. 33, (1977), p. 45-54.
2. J. Chevrier, M. Armand, A.M. Huber and Nuyen T. Link, "Vapor Growth of InP for MESFET's", Journal of Electronic Material, 9, 4, (1980), p. 745-761.
3. T.J. Maloney and J. Frey, "Frequency Limits of GaAs and InP Field Effect Transistors at 300 K and 77 K with Typical Active Layer Doping", IEEE Transactions on Electronic Devices, ED 23, 519 (1976).
4. R.C. Clarke, "Indium Phosphide Vapor Phase Epitaxy: A Review", Journal of Crystal Growth 54 (1981), 88-100.
5. R.C. Clarke and L.L. Taylor, "Multilayered Structures of Epitaxial Indium Phosphide," Journal of Crystal Growth 31 (1975) 190-196.
6. P. Moutou, J. Chevrier, A. Huber and J. Montel, "Vapor Epitaxial Growth and Characterization of InP Millimeter-wave Oscillators", Institute of Physics Conference Series No. 45, Chapter 5, 452-461 (1979).
7. H. Morkoc, J. Andrews, S.B. Hyder and S.G. Bandy, "InP MESFET's prepared by VPE", Institute of Physics Conference See No. 45, Chapter 4, 295-300 (1979).

8. R.C. Clarke, B.D. Joyce and W.H.E. Wilgors, "The Preparation of High Purity Epitaxial InP", Solid State Communications 8, 1125 (1970).

9. A. Christou and W.T. Anderson, Jr. "Deposition of Thin Refractory MD Structures on InP", Journal of Electronic Material 9, No. 3 (1980), p. 585-599.

10. D.V. Morgan, M.J. Hower and W.J. Devlin, "A study of gold In-InP contacts", Journal of Physics D: Applied Physics, Vol. II, (1978), 1341-1350.

11. R.H. Williams, V. Montogeny and R.R. Varma, "Chemical effects in Schottky barrier formation," Journal of Physics C: Solid State Physics II (1978), L735-L738.

12. D.V. Morgan and J. Firey, "Schottky Barrier Height: A Design Parameter for Device Applications," Solid State Electronics 22 (1979) 865-873.

13. A Christou and W.T. Anderson, Jr. "Material Reactions and Barrier Height Variations in Sintered Al-InP Schottky Diodes," Solid State Electronics 22 (1979), 857-863.

14. G.G. Roberts and K.P. Pande, "Electrical characteristics of Au/Tl-(n type) InP Schottky diodes", Journal of Physics D: Applied Physics 10 (1977), 1323-1328.

15. D.K. Skinner, "New Method of Preparing (100) InP Surfaces for Schottky Barrier and Ohmic Contact Formation", Journal of Electronic Material Vol. 9, No. 1 (1980), 67-78.

16. R.H. Williams, R.R. Varma, and A. McKinley, "Cleaved surfaces of indium phosphide and their interfaces with metal electrodes", Journal of Physics C: Solid State Physics 10, (1977), 4545-4557.

17. S. Von Rump, G. Homsey, M. Reese, and J. Bornholdt, "System for the measurement of transport properties of semiconductors", ONR Report-80-1, 1980.

18. J. Teng, R.E. Goldwasser, VPE Growth of GaAs, ONR Report-80-1, 1980.

19. R. Green, "Vapor Phase Epitaxial Growth", Master's Thesis, Washington University, 1980.

20. R.N. Hall, "Solubility of III-V Compound Semiconductors in Column III Liquids," Journal of the Electrochemical Society 110, No. 5, 385 (1963).

21. C.D. Hodgman, Handbook of Chemistry and Physics, The Chemical Rubber Publishing Co., Cleveland, Ohio, 2437, (1963).

22. R.C. Clarke, "Chemistry of the In-H_2-PCl_3 Process," Inst. Phys. Conf. Ser. No. 45, Chp. 1, 1979, 21.

23. R.C. Weast, Handbook of Chemistry and Physics, The Chemical Publishing Co., Cleveland, Ohio, 1972.

24. J. Chevrier, A. Huber and N.T. Lin, "Vapor Phase Epitaxy of InP: Growth kinetics and controlled doping," Journal of Crystal Growth 47 (1979), 267-273.

25. A van der Zeil, Solid State Physical Electronics, 3rd edition, Prentice-Hall Inc., Englewood Cliffs, NJ (1976).

26. P.C. Clarke and L.L. Taylor "Pure and Doped InP by VPE", Journal of Crystal Growth 43, 473 (1978).

27. W.E. Spicer, P.W. Chye, C.M. Garner, I. Lindau, and P. Pianetta, "The surface electronic structure of 3-5 compounds and the mechanism of Fermi level pinning by oxygen (passivation) and metals (Schottky barriers)", Surface Science 86 (1979) 763-788.

28. A.R. Clawson, D.A. Collins, D.I. Eldar, J.J. Monroe, "Laboratory Procedures for Etching and Polishing InP Semiconductor", NOSC Technical Note 592, Dec. 13, 1978.

29. Y. Nishitani and T. Kotani, "Chemical Etching of InP by H_2O_2-H_2SO_4-H_2O Solution", Journal of the Electrochemical Society: Solid State Science and Technology 126, No. 12, pp. 2269-2271 (1979).

DISTRIBUTION LIST
CONTRACT N00014-79-C-0840

Code 414 — 4
Office of Naval Research
Arlington, VA 22217

Naval Research Laboratory
4555 Overlook Avenue, S.W.
Washington, D.C. 20375
Code 6811 — 1
6850 — 1
6820 — 1
6851 — 1

Defense Documentation Center — 12
Building 5, Cameron Station
Alexandria, VA 22314

Dr. Y. S. Park — 1
AFWAL/DHR
Building 450
Wright-Patterson AFB
Ohio 45433

Texas Instruments — 1
Central Research Lab
M.S. 134
13500 North Central Expressway
Dallas, TX 75265
ATTN: Dr. W. Wisseman

Dr. R. M. Malbon/M.S. 1C — 1
Avantek, Inc.
3175 Bowers Avenue
Santa Clara, CA 94304

Dr. R. Bierig — 1
Raytheon Company
28 Seyon Street
Waltham, MA 02154

Dr. Mike Driver — 1
Westinghouse Research and
Development Center
Beulah Road
Pittsburgh, PA 15235

Dr. F. Eisen — 1
Rockwell International
Science Center
P.O. Box 1085
Thousand Oaks, CA 91360

Dr. C. Krumn — 1
Hughes Research Laboratory
3011 Malibu Canyon Raod
Malibu, CA 90265

Mr. Lothar Wandinger — 1
ECOM/AMSEL/TL/IJ
Fort Monmouth, NJ 07003

Dr. William Lindley — 1
MIT
Lincoln Laboratory
F124 A, P.O. Box 73
Lexington, MA 02173

Commander — 1
U.S. Army/ERADCOM
ATTN: V. Gelnovatch, DELET-M
Fort Monmouth, NJ 07703

RCA — 1
Microwave Technology Center
Dr. F. Sterzer
Princeton, NJ 08540

Commander — 1
Naval Electronics Systems Command
ATTN: J. P. Letellier, Code 6142
Washington, D.C. 20360

Commander — 1
Naval Air Systems Command
ATTN: A. Glista, Jr., AIR 34
Washington, D.C. 20361

Dr. R. Bell, K-101 — 1
Varian Associates, Inc.
611 Hansen Way
Palo Alto, CA 94304

Hewlett-Packard Corporation 1
Dr. Robert Archer
1501 Page Road
Palo Alto, CA 94306

Watkins-Johnson Company 1
E. J. Crescenzi, Jr./
K. Niclas
3333 Hillview Avenue
Stanford Industrial Park
Palo Alto, CA 94304

Commandant 1
Marine Corps
Scientific Advisor (Code AX)
Washington, D.C 20380

Communications Transistor Corp. 1
Dr. W. Weisenberger
301 Industrial Way
San Carlos, CA 94070

Microwave Associates 1
Northwest Industrial Park
Drs. F. A. Brand/J. Saloom
Burlington, MA 01803

Commander, AFAL 1
AFWAL/AADM
Dr. Don Rees
Wright-Patterson AFB, OH 45433

Professor Walter Ku 1
Phillips Hall
Cornell University
Ithaca, NY 14853

Commander 1
Harry Diamond Laboratories
Mr. Horst W. A. Gerlach
800 Powder Mill Road
Adelphia, MD 20783

A.G.E.D. 1
201 Varick Street
9th Floor
New York, NY 10014

Dr. Ken Weller 1
MS/1414
TRW Systems
One Space Park
Redondo Beach, CA 90278

Professor L. Eastman 1
Phillips Hall
Cornell University
Ithaca, NY 14853

Professor Hauser and 1
Littlejohn
Department of Electrical Engr.
North Carolina State University
Raleigh, NC 27607

Professor J. Beyer 1
Department of Electrical and
Computer Engineering
University of Wisconsin
Madison, WI 53706

W. H. Perkins 1
Electronics Lab 3-115/B4
General Electric Company
P.O. Box 4840
Syracuse, NY 13221

Bryan Hill 1
AFWAL/AADE
Wright-Patterson AFB, OH 45433

H. Willing/Radar Directorate 1
BMD - Advanced Technical Center
P.O. Box 1500
Huntsville, AL 35807